Modeling of Biomass Gasification with Adaptation to Biological Methanation Using Aspen Plus®

by

Abdallah Almashharawi

Department of Chemical Engineering
Lund University
&
RISE AB

January 2022

Supervisor (LTH): **Professor Ola Wallberg**
Co-supervisor (RISE): **Senior Researcher Anders Wingren**
Examiner (LTH): **Senior Lecturer Mats Galbe**

Postal address	**Visiting address**	**Telephone**
P.O. Box 124	Naturvetarvägen 14	+46 46-222 82 85
SE-221 00 Lund, Sweden		+46 46-222 00 00
Web address		**Telefax**
www.lth.se/chemeng/		+46 46-222 45 26

بِسْمِ اللَّهِ الرَّحْمَٰنِ الرَّحِيمِ

Preface

All thanks and praise are due to Allah, whom we seek His help and forgiveness. Thanks to Allah, Almighty, for all favors upon us.

I would like to express my deepest gratitude to my family for their support during my studies. My wife Iman and my son Ismael, you are the light of my life and the source of my happiness. It has been tough years with many challenges along the way, but together we have managed through them. To my mother and father, thank you for all the sacrifices you have made for me and my siblings.

I would like to thank my supervisors Ola Wallberg and Anders Wingren, my examiner Mats Galbe, and Johan Andersson at RISE for all the support during this master thesis project. I would also like to thank my friend Omar Abdelaziz for reviewing this report and my brother-in-law Khoder El Saleh for proofreading my Arabic summary. I would like to thank all the teachers I have had; you do a great job of educating the new generation of the future. Finally, I would like to thank all the friends I have met during my studies, these years would have been boring without you.

This master's thesis project has been performed at the Department of Chemical Engineering at Lund University. The work was carried out in collaboration with Meva Energy AB and RISE AB, where Meva Energy AB is the technology owner for the gasification process and RISE AB is the research partner focusing on biological methanation.

Abstract

With reduced resources of fossil fuels and increased environmental requirements, renewable substitutes have received greater attention. The production of renewable chemicals and fuels through biomass gasification presents a promising route to drive this energy transition. Synthesis gas (syngas), a mixture of mainly CO and H_2, can be produced from biomass via gasification. Biological methanation, as a potential alternative to catalytic methanation, can then be used to produce biogas from biomass-derived syngas.

The aim of this work was to model the gasification process of biomass in the Aspen Plus® simulation software with an adaptation to the subsequent biological methanation of syngas. The study was based on Meva Energy's 5-MW_{th} cyclone gasifier, which operates at 0.65 barg and 850–1000 °C. The generated syngas consisted mainly of N_2, H_2, CO, CO_2, CH_4, light non-aromatic hydrocarbons, and tars.

As of today, most simulations found in literature using Aspen Plus® are based on equilibrium calculations. The main drawbacks of equilibrium-based models are the overestimation of char conversion and the neglect of tars and their reactions during gasification. In this study, equilibrium and kinetic models were developed for modeling biomass gasification in a cyclone gasifier. In addition, a third model was developed for the succeeding gas-cleaning system in the plant. All models were validated against experimental data. The lower heating value of produced gas and the cold gas efficiency of the process were calculated for all cases.

Predicted temperature in the gasifier was lower than experimental data when equilibrium was assumed. A large deviation was also observed between the equilibrium model and measurements with respect to concentrations of H_2, CH_4 and light non-aromatic hydrocarbons. On the other hand, a better agreement between simulation and experimental data was found when employing the kinetic-based model. When validating the gas-cleaning model, predicted values showed some agreement with measurements, but big errors were observed for some components, such as indene and naphthalene.

For the biological methanation process, the main requirement is a syngas free of N_2. There is no negative effect of N_2 on the biological methanation itself, however, the separation of N_2 in the product can be associated with high costs. This requirement can be achieved by replacing air as the gasification medium with a mixture of O_2 and recycled CO_2 which has been separated from the gas after the methanation. When gasification was adapted to biological methanation, a lower gasification temperature was observed compared to conventional air-blown gasification at the same air–fuel equivalence ratio (lambda). This comes with a cost of lower cold gas efficiency and higher tar content in the syngas. Therefore, lower concentration of CO_2 in the gasifying medium is desired, but particle separation will be affected as the gas volumetric flow rate decreases.

Sammanfattning

Med minskade resurser av fossila bränslen och ökade miljökrav har förnybara ersättningar fått större uppmärksamhet. Produktionen av förnybara kemikalier och bränslen genom förgasning av biomassa är en lovande lösning för att driva denna energiomställning. Syntesgas (syngas), en blandning av främst CO och H_2, kan framställas av biomassa via förgasning. Biologisk metanisering, som ett potentiellt alternativ till katalytisk metanisering, kan sedan användas för att framställa biogas från syngas som härrör från biomassa.

Syftet med detta arbete var att modellera förgasningsprocessen av biomassa i simuleringsmjukvaran Aspen Plus® med en anpassning till den efterföljande biologiska metaniseringen av syngas. Studien baserades på Meva Energys 5-MW_{th} cyklonförgasare, som arbetar vid 0.65 bar övertryck och 850–1000 °C. Den producerade syngasen bestod huvudsakligen av N_2, H_2, CO, CO_2, CH_4, lätta icke-aromatiska kolväten samt tjäror.

Av de simuleringar i Aspen Plus® som finns publicerade i litteraturen idag, så är de flesta baserade på jämviktsberäkningar. De främsta nackdelarna med jämviktsbaserade modeller är överskattningen av kolomsättningen och försummelsen av tjäror och deras reaktioner under förgasningen. I denna studie har jämvikts- och kinetiska modeller utvecklats för att modellera biomassaförgasning i en cyklonförgasare. Dessutom utvecklades en tredje modell för att simulera det efterföljande gasreningssystemet i anläggningen. Alla modeller validerades mot experimentella data. Det effektiva värmevärdet för producerad gas och processens verkningsgrad beräknades för samtliga fall.

Den predikterade temperaturen i förgasaren var lägre än det uppmätta värdet när jämvikt antogs. En avvikelse observerades också mellan jämviktsmodellen och mätningar med avseende på koncentrationer av H_2, CH_4 och lätta icke-aromatiska kolväten. Däremot uppnåddes en bra överensstämmelse mellan simuleringen och experimentella data när man använde den kinetikbaserade modellen. Vid validering av gasreningsmodellen visade predikterade värden en god överensstämmelse med mätningar, men stora avvikelser observerades för vissa tjärkomponenter t.ex. indene och naftalen.

För den biologiska metaniseringen är huvudkravet en syngas fri från N_2. Ingen negativ effekt av N_2 finns på den biologiska metaniseringen i sig, dock kan separationen av N_2 i produkten vara förknippad med höga kostnader. Detta krav kan uppnås genom att byta ut luft som förgasningsmedium mot en blandning av O_2 och recirkulerad CO_2 som man har avskilt från gasen efter metaniseringen. När förgasningen anpassades till biologisk metanisering observerades en lägre förgasningstemperatur jämfört med konventionell luftblåst förgasning vid samma luft-bränsle-förhållande (lambdavärde). Detta kommer med en kostnad av en lägre verkningsgrad på processen och högre tjärhalt i syngasen. Därför är lägre koncentration av CO_2 i förgasningsmediet önskvärt, däremot kommer partikelseparationen att påverkas när gasens volymflöde minskar.

Arabic summary (الملخص العربي)

حظيت البدائل المتجددة باهتمام كبير في ظل انخفاض موارد الوقود الاحفوري المتاحة وزيادة المتطلبات البيئية. ان انتاج المواد الكيميائية والوقود المتجدد من خلال استغلال الكتلة الحيوية يقدم طريقا واعدا لدفع هذا التحول الى الامام. ومن الممكن انتاج غاز "الاصطناع" (syngas)، وهو خليط مكون أساسا من غاز اول أكسيد الكربون (CO) وغاز الهيدروجين (H_2)، من الكتلة الحيوية عبر عملية التغويز (gasification). يمكن بعد ذلك استخدام عملية انتاج الميثان البيولوجية (biological methanation) كبديل محتمل للعمليات التحفيزية لإنتاج الغاز الحيوي من غاز "الاصطناع" المشتق من الكتلة الحيوية.

كان الهدف من هذا المشروع نمذجة ومحاكاة عملية تغويز الكتلة الحيوية في برنامج المحاكات Aspen Plus® مع التكيف لعلمية انتاج غاز الميثان بطريقة بيولوجية. استندت هذه الدراسة على مفاعل التغويز الدوّامي (cyclone gasifier) بقدرة 5 ميجاواط حرارية التابع لشركة Meva Energy والذي يعمل تحت ضغط 0.65 barg ودرجة حرارة ما بين 850 و1000 درجة مئوية. يتكون الغاز الناتج بشكل أساسي من النيتروجين (N_2)، والهيدروجين (H_2)، وأول أكسيد الكربون (CO)، وثاني أكسيد الكربون (CO_2)، والميثان (CH_4)، والهيدروكربونات الخفيفة غير العطرية (non-aromatic)، والقطران (tars).

انّ معظم الدراسات المنشورة حالياً حول نماذج المحاكاة التي تستخدم برنامج Aspen Plus® تسند على استخدام حسابات التوازن الكيميائي. لكنّ هذه الحسابات تتسم غالباً في المبالغة في تقدير مدى تفاعل الكربون وإهمال وجود القطران أثناء عملية التغويز. في هذه الدراسة تم تطوير نماذج تستند على التوازن الكيميائي وسرعة التفاعلات الكيميائية لعملية تغويز الكتلة الحيوية في المفاعل الدوّامي. بالإضافة إلى ذلك، تم تطوير نموذج لنظام تنظيف الغاز التابع لهذا المفاعل، ثم تم التحقق من صحة جميع النماذج باستخدام بيانات وقياسات حقيقية من المفاعل. تم أيضاً حساب قيمة حرارة الاحتراق الدنيا (lower heating value) للغاز الناتج وكفاءة العملية (cold gas efficiency) لجميع الحالات.

كانت درجة الحرارة المتوقعة في المفاعل أقل بكثير عند استخدام نموذج التوازن الكيميائي مقارنة بالبيانات الحقيقية. كما لوحظ انحراف كبير بين نموذج التوازن والقياسات الحقيقة بالنسبة لتركيزات غاز الهيدروجين (H_2) والميثان (CH_4) والهيدروكربونات الخفيفة غير العطرية. ومن ناحية أخرى، تم العثور على اتفاق جيد بين المحاكاة والبيانات التجريبية عند استخدام النموذج القائم على سرعة التفاعلات الكيميائية. عند التحقق من صحة نموذج تنظيف الغاز، أظهرت النتائج المتوقعة بعض التوافقات مع القياسات الحقيقية، ولكن لوحظ وجود تباينات كبيرة في تركيز بعض المكونات مثل الإندين (indene) والنفثالين (naphthalene).

بالنسبة لعملية انتاج الميثان البيولوجية، فإن الشرط الرئيسي هو استخدام غاز "الاصطناع" (syngas) خالٍ من غاز النيتروجين (N_2). ولم يتم العثور على اي تأثير سلبي لغاز النيتروجين على عملية انتاج الميثان البيولوجية بذاتها، ولكن تكمن الإشكالية في ان عملية فصل غاز النيتروجين من المنتج تكون ذو تكلفة عالية. يمكن تحقيق هذا الشرط الرئيسي عن طريق استخدام مزيج من غاز الاكسجين (O_2) وثاني أكسيد الكربون (CO_2) بدلاً من الهواء خلال عملية التغويز. وعندما تم تغيير عملية التغويز لتناسب عملية انتاج الميثان البيولوجية، لوحظ انخفاض في درجة حرارة المفاعل مقارنة بعملية التغويز التقليدية. ويتسبب هذا التغيير في انخفاض كفاءة عملية التغويز وفي زيادة محتوى القطران في الغاز الناتج. لذلك يعد استخدام تركيز منخفض من غاز ثاني أكسيد الكربون (CO_2) في وسط التغويز (gasifying medium) أمرًا مرغوبًا فيه، ولكن هذا سيؤثر في كفاءة عملية فصل الجسيمات من الغاز الناتج بسبب انخفاض معدل التدفق الحجمي للغاز.

Contents

1 Introduction 1
2 Theory 2
2.1 General description of the facility 2
2.2 Chemical processes in gasifier 3
2.3 Biological methanation of syngas 5
3 Literature review 6
4 Methods 7
4.1 Equilibrium-based gasification model 7
4.2 Combined equilibrium-based and kinetic-based gasification model with pyrolysis correlations 11
4.3 Modification of gasifier models for adaptation to biological methanation 14
4.4 Gas-cleaning system model 16
5 Results and discussion 21
5.1 Validation of equilibrium-based gasification model 21
5.2 Validation of combined equilibrium-based and kinetic-based gasification model 23
5.3 Validation of gas-cleaning system 29
5.4 Adaptation of gasification process to subsequent biological methanation 31
6 Conclusions 37
6.1 Future work 38
7 References 39
8 List of abbreviations 42

1 Introduction

With reduced resources of fossil fuels and increased environmental requirements, renewable substitutes have received greater attention. Methane gas can be produced from syngas in a process called biological methanation. Depending on its composition, this gas can be used in transport sector or in industry replacing fossil fuels. For this to be possible, the gasification process must be adapted to this application.

Meva Energy AB, founded in 2008 in Sweden, is a provider of gasification technology that supplies systems that can use biomass to produce renewable electricity and heat. The company has developed a gasification process of wood powder for the production of syngas in both pilot and demo scale [1].

The aim of this study is to model the biomass gasification process in Aspen Plus® simulation software with an adaptation of the gasifier to the subsequent intended biological methanation of syngas. Both the gasifier and the subsequent gas-cleaning system are going to be modeled and simulated. Furthermore, all models are going to be validated against experimental data. These data were collected at the plant by measurements done in previous studies and received by company supervisor at Meva Energy AB.

No comprehensive optimization of the process adaptation to biological methanation will be conducted due to the time limitation of this study. However, some criteria are set up on the process according to input from the methanation project group at RISE.

The following research questions are answered in this study:

- How is biomass gasification modeled and simulated in literature?
- How can biomass gasification be modeled and simulated using Aspen Plus®?
- How well do results from the developed model agree with experimental data?
- What changes are needed to adapt biomass gasification to the biological methanation of syngas?

The project was divided into the following parts based on the defined research questions:

- Literature study on how gasification was modeled and simulated previously
- Collection of process flow diagrams, technical specifications, and process data
- Modeling of the process in Aspen Plus®
- Validation of the model with data from the demonstration plant
- Process adaptation to the biological methanation of syngas

2 Theory

2.1 General description of the facility

This study was based on Meva's 5-MW_{th} demonstration plant in Hortlax, Sweden. Process flow diagrams and measurement data from the operational units of the plant were received by co-supervisor. The block flow diagram of the plant is shown in Figure 2.1. Here, the operational units included in this study are represented in solid line, and the excluded parts of the plant in dashed line [2].

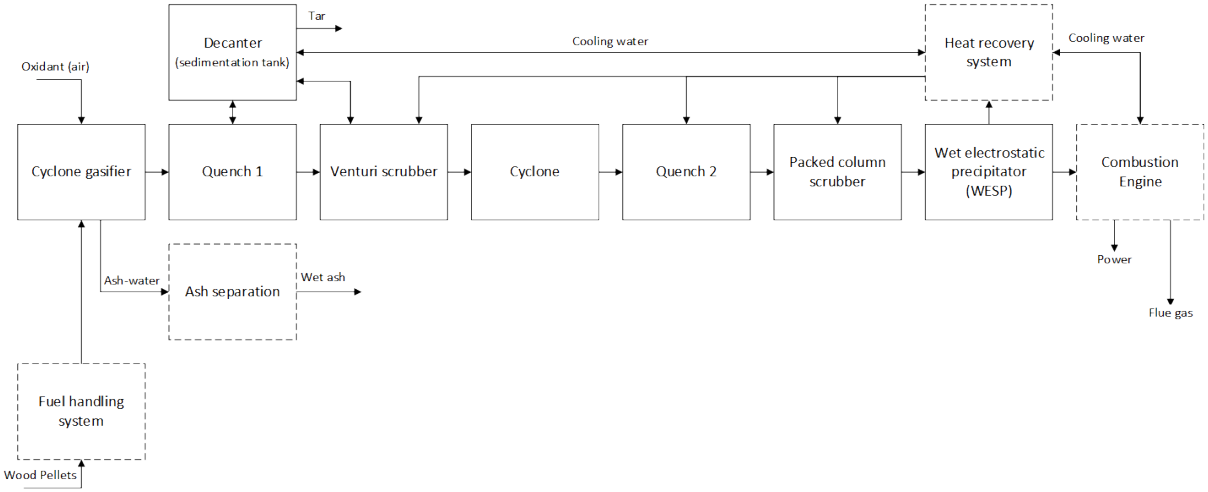

Figure 2.1. Block flow diagram of Meva's facility. The operational units studied are shown in solid lines, and the excluded parts of the plants are outlined in dashed lines.

Virgin wood pellets from *Pinus sylvestris* and *Picea abies* are supplied as fuel to the fuel handling system where the pellets from a silo are screwed to a grinder at a flow rate of 800–1000 kg/h. Pellets after the grinder are blown into the cyclone gasifier as a fine powder. Air is used as gasifying agent and carrier medium for the powder with an air–fuel equivalence ratio (lambda) of about 0.3. The gasifier is an entrained flow cyclone gasifier with height of 3 m, internal diameter of 0.75 m and internal insulation made of ceramic [2].

An oil burner is used initially to preheat the cyclone gasifier to about 800 °C, this is only done in the beginning of the operation until correct temperature is reached. A mixture of air and fuel is then supplied to the cyclone gasifier through blowers into two inlets at the top at an inlet velocity of 30–50 m/s. The cyclone gasifier is operated at a pressure of about 0.65 barg and a gas temperature range of 850–1000 °C.

The produced wet syngas consisting mainly of N_2, H_2, CO, CO_2, CH_4, light non-aromatic hydrocarbons C_xH_y and tars, leaves the cyclone gasifier through a vortex finder from the top. The part of the fuel that does not form gas, called char, is collected at the bottom of the cyclone gasifier together with the produced ash where the temperature can reach up to 1200 °C. Before char collection, a secondary air flow of about 50 kg/h is supplied to the bottom of the cyclone gasifier to further increase the conversion of char. Due to the presence of reducing zones in the cyclone gasifier, components such as H_2S, COS, NH_3, HCN and alkaline compo-

nents can be found in the product gas. Type of contaminants and their concentrations in the product gas depends among other things on which fuel is used for gasification. Moreover, many trace elements can be found in produced char in the bottom [2].

As shown in Figure 2.1, the produced gas is then cleaned and cooled through several stages in the gas-cleaning system. The first step is a water quench where water is sprayed into the gas reducing its temperature to about 84 °C, allowing condensation of heavy tars. Wet gas is then led through a venturi scrubber where particles and soot are separated with the supplied water. A cyclone with a height of 3.5 m and internal diameter of 0.8 m is then used to further separate particles from the gas.

A second water quench reduces the gas temperature further to about 60 °C. A column filled with metallic random packing is then used to scrub the gas with water and cool it to about 40 °C. These units allow condensation of water vapor and cleaning the gas of tars and soot. Finally, the gas flows through a wet electrostatic precipitator (WESP) consisting of vertical tubes with high-voltage direct current. This unit separates small particles and tar aerosols from the gas before the subsequent engine combustion or synthesizes [2].

Contaminated process water from all operating units is produced, therefore a decanter (sedimentation tank) is used in a closed water circuit providing clean water. Heavy tars and soot fall to the bottom of the sedimentation tank, then clean process water is cooled in the heat recovery system. Char from the bottom of the cyclone gasifier is collected and handled in a separate wet char handling system. Water is used to cool the char, then a drum filter is used to separate the char from water.

2.2 Chemical processes in gasifier

Gasification can be described as a partial combustion, i.e., a combustion that takes place in the deficit of oxygen. The gasification of fuel consists mainly of four processes, which are drying, pyrolysis, oxidation, and reduction. All processes occur simultaneously during the residence time of less than a few seconds in the cyclone gasifier. Most important factors affecting the reaction rates are gasifier temperature and particle size distribution of fuel particles [3].

Initially, fuel particles are heated, and water is vaporized when the temperature is high enough. Further heating results in the beginning of the pyrolysis or devolatilization process of fuel particles. This process releases volatile matter of the particles producing gases, pyrolysis oil, tars, and char. The pyrolysis products mainly consist of CO, CO_2, H_2, H_2O, CH_4, light non-aromatic hydrocarbons and tars. The produced char consists mainly of carbon and ash. Tar is a complex mixture of many aromatic compounds such as benzene, toluene, xylene, styrene, phenol, indene, naphthalene, anthracene, pyrene and up to coronene. Pyrolysis product composition and yield depends highly on gasifier temperature and composition of fuel [3, 4].

The product of pyrolysis undergoes both homogeneous gas phase reactions and heterogeneous reactions. Homogeneous reactions include oxidation (combustion) with oxygen providing heat required to maintain temperature of the gasifier and to the endothermic reactions. Other homogeneous reactions include reactions with water vapor such as water-gas shift reaction and cracking reactions of tars. Heterogeneous reactions include gasification of char with O_2, H_2O and CO_2. Heterogeneous reactions of char with H_2O and CO_2 are slow relative other re-

actions. These occur mostly in the bottom of the gasifier where char is collected, and the residence time is several minutes with injection of secondary air [3].

Table 2.1 shows main reactions considered in this gasifier. No reactions of tars other than benzene are shown in the table due to the complex nature of these reactions [3]. Enthalpies of reactions were calculated for demonstration purpose in Aspen Plus®, assuming stoichiometric reactions at 1 atm and 25 °C.

Table 2.1. Main reactions involved in the gasification process with enthalpy of reaction (kJ/mol) calculated in Aspen Plus® at 1 atm and 25 °C.

No.	Reaction	Enthalpy of reaction at 1 atm and 25 °C (kJ/mol)
Homogeneous gas phase reactions		
1	$CH_4 + 1.5\ O_2 \rightarrow CO + 2\ H_2O$	-520
2	$CH_4 + H_2O \rightarrow CO + 3\ H_2$	206
3	$C_2H_4 + 2\ O_2 \rightarrow 2\ CO + 2\ H_2O$	-757
4	$H_2 + 0.5\ O_2 \rightarrow H_2O$	-242
5	$CO + 0.5\ O_2 \rightarrow CO_2$	-283
6	$CO + H_2O \rightarrow CO_2 + H_2$	-41
7	$C_6H_6 + 4.5\ O_2 \rightarrow 6\ CO + 3\ H_2O$	-1472
8	$C_6H_6 + 6\ H_2O \rightarrow 6\ CO + 9\ H_2$	706
Heterogeneous reactions		
9	$C_{(s)} + 0.5\ O_2 \rightarrow CO$	-111
10	$C_{(s)} + H_2O \rightarrow CO + H_2$	131
11	$C_{(s)} + CO_2 \rightarrow 2\ CO$	172

Considering reactions of tars, as temperature increases more tars are cracked becoming less branched and with less oxygen content. Many side reactions between tars can also occur such as production of polycyclic aromatic hydrocarbons (PAHs). At even higher temperatures, around 1000 °C, more soot is produced in the gasifier. Soot production is usually a problem inside the gasifier, but tar production is more problematic to the gas-cleaning system [2, 5].

2.3 Biological methanation of syngas

Biogas is a gas mixture of mainly CH_4 and CO_2 with smaller amounts of N_2, H_2 and contaminants, such as sulfur compounds. Depending on its composition, it can be used in the transport sector or in the industry sector replacing fossil fuels [6].

Biogas can be methanized biologically via operation of continuous methanation processes. This pathway of producing biogas is expected to be more cost-efficient relative conventional catalytic processing of syngas [7, 8].

For the biological methanation process studied, the main requirement is a syngas free of N_2. No negative effect of N_2 is found on the biological methanation itself, however, separation of N_2 in the final biogas is a process with high costs. This requirement can be achieved by gasification with only O_2, or a mixture of O_2 and recirculated CO_2 instead of air, and sometimes with addition of steam [8]. However, by using pure O_2 a too high temperature in the gasifier would be reached. This would among other things cause melting of ash. Apart from that, gas physical properties would also change significantly which may affect particle separation efficiency of the cyclone gasifier [2].

Optimal proportions of H_2, CO and CO_2 in the syngas for biological methanation are dependent on its content of CH_4. If the syngas has no CO_2 or CH_4, then the optimal ratio H_2:CO is 3:1. If the syngas contains CO_2, then every mole of CO_2 requires 4 moles of H_2 to produce CH_4 and H_2O. Higher H_2 concentration is desired as H_2 is used as an energy source for metabolism of the microorganisms, transforming CO2 to CH_4. A higher CH_4 concentration is also desired as this would decrease load on the process as CH_4 would flow through the process without further conversion [8, 9].

Fortunately, the process can handle a wide range of syngas compositions if optimal proportions are not possible to reach. When all CO and H_2 in the syngas are consumed the gas consists mainly of CH_4 and CO_2. One approach is then to separate CO_2 in the subsequent purification steps to reach a high fraction of CH_4. Alternatively, more H_2 is added to the methanation via an electrolysis process and thus more CO_2 is converted [8].

Some contaminants in the syngas, such as NH_3 and H_2S, are favorable for nutrition of the microorganisms, others such as HCN are not due to its toxic effects. Benzene and other heavier hydrocarbons might be difficult to handle in the methanation process; therefore, its concentration should be minimized in the syngas if further experiments confirm its negative effect. High concentration of these contaminants involves higher investment and operating costs due to requirement of additional energy and operation units in the gas-cleaning system. Temperature of the syngas itself should be within the interval of 50–100 °C after the gas-cleaning system. Furthermore, particle concentration in the syngas might have a negative effect on handling of the nutrient solution afterwards. However, further experiments are required to confirm this effect [8, 10].

3 Literature review

Gasification of biomass and coal is widely studied in literature with several studies using Aspen Plus® to simulate this process [11-21]. However, to the best of the author's knowledge, only one study could be found in the literature which simulated the process based on experimental data from a cyclone gasifier [22]. Most of Aspen Plus® simulations were found to be based on the Gibbs minimization equilibrium approach using either RGIBBS or REQUIL as a reactor block. A thorough review on the progress of biomass gasification simulation in Aspen Plus® was conducted in literature, which confirms this observation [23].

The equilibrium-based approach is easier as it does not require input of reaction kinetics or equations as required for kinetic models using RCSTR or RPlug. The main drawbacks of equilibrium-based modeling are overestimation of char conversion, and neglect of tars and their reactions. Another drawback is that equilibrium-based models do not take any consideration to reactor design and configuration, as these models assumes infinite time of reaction to reach equilibrium. The most convenient way to utilize equilibrium-based models is to study the effects of operating conditions such as temperature, pressure and concentration on product yields and thermodynamic limitations of the process [23].

A different approach is to combine equilibrium and kinetic models in the same simulation. In this approach, some reactions could be assumed to follow equilibrium when kinetic data are not available. Furthermore, Aspen Plus® models can be combined with models developed in MATLAB, FORTRAN, or other programming languages. This approach provides models necessary to simulate chemical and physical processes in the gasifier when Aspen Plus® standard models are not satisfying [23].

Regardless of the approach used, some assumptions must be made to be able to model this process. Most models were found to assume these general assumptions [23]:

- Steady-state and isothermal process
- Instant drying and pyrolysis of biomass
- Perfect mixing giving uniform composition, temperature, and pressure
- Ash is inert
- Char consists of only carbon and ash
- No catalytic effects are considered

Another approach to simulate gasification processes is via computational fluid dynamic (CFD) modeling. This approach was done in some studies, including a study done on the same cyclone gasifier at Meva Energy in Hortlax, Sweden [3, 24-27]. The most important benefit of CFD modeling is its ability in simulating complex fluid dynamics and heat transfer processes considering dimensions of the vessel. However, CFD models are relative complex and require relative long computation time. Moreover, Aspen Plus® provides an extensive database of compounds with several physical methods models providing more accurate calculation of physical properties [28]. Benefits of these two approaches combined have led to combine CFD models with physical properties obtained from Aspen Plus® databases in their simulations [29, 30].

4 Methods

Two main models were developed for the simulation of biomass gasification in a cyclone gasifier using Aspen Plus® V10. Furthermore, one model was developed for the succeeding gas-cleaning system in the plant.

The first gasification model is a simple equilibrium model mainly based on minimization of Gibbs free energy in a RGIBBS block. The second model is more advanced, considering some reactions kinetics in a RCSTR block with correlations of the pyrolysis step in a RYield block. A modification to the models was made after simulating the base case to adapt the process to the subsequent biological methanation process.

The base case is the setup with air as gasifying medium which the models are validated against. Measurements from the base case are presented in section 5. Furthermore, validation of the gasifier models was done on the effect of temperature variation and fuel moisture content variation.

The lower heating value (LHV) in MJ/Nm^3 of the produced gas and cold gas efficiency (CGE) of the process were calculated for all gasification models. These are important parameters used when performance of gasification processes is studied. This was done with reference at 25 °C and 1 atm using a RSTOIC block in Aspen Plus®. A stoichiometric flow of oxygen was calculated by a calculator block, assuming complete combustion of CO, H_2, CH_4, C_2H_4 and C_6H_6 giving H_2O and CO_2 as products. LHV of the gas was calculated by subtraction of heat required to vaporize the water in the flue gas from the heat produced by the combustion reactions Q_{RSTOIC}. The enthalpy of vaporization of water ΔH_{vap} was set constant and chosen at 25 °C and 1 atm to 2.442 MJ/kg [31].

$$LHV_{gas} = \frac{|Q_{RSTOIC}| - \dot{m}_{H2O}\Delta H_{vap}}{\dot{V}_{gas}} \quad (1)$$

When calculating CGE of the process, the gas volumetric flow rate $\dot{V}_{gas}$ is calculated at 25 °C and 1 atm. The fuel $LHV_{F,db}$ is given by analysis of virgin wood pellets on dry basis (db) and has the value of 19.43 MJ/kg dry biomass [2]. Both LHV and CGE were calculated including tars for all cases.

$$CGE = \frac{\dot{V}_{gas}\, LHV_{gas}}{\dot{m}_{F,db}\, LHV_{F,db}} \quad (2)$$

4.1 Equilibrium-based gasification model

The components defined in this model are given in Table 4.1. The property methods suitable to define nonconventional components are HCOALGEN and DCOALIGT. These property methods were developed for coal but are considered suitable for biomass according to the Aspen Plus® User Guide. Option codes defined are 1 1 1 1 for ASH and 6 1 1 1 for BIOMASS, which enables using the measured higher heating value (HHV) on dry basis of biomass as input [32]. For biomass used in the studied plant, a HHV of 20.79 MJ/kg dry biomass was used according to analysis [2].

For physical property calculations, one suitable property method is Peng–Robinson cubic equation of state with the Boston–Mathias alpha function (PR-BM) according to the Aspen Plus® methods assistant. Moreover, many studies found on biomass gasification in Aspen Plus® used the same property method [23]. The used stream class was set to MCINCPSD as conventional and nonconventional solids were used with a defined particle size distribution (PSD).

Table 4.1. Components defined for the equilibrium-based gasification model in Aspen Plus®.

Component	Type	Component	Type
BIOMASS	Nonconventional	CH_4	Conventional
ASH	Nonconventional	C_2H_2	Conventional
C	Solid	C_2H_4	Conventional
S	Conventional	C_6H_6	Conventional
N_2	Conventional	NO_2	Conventional
O_2	Conventional	NO	Conventional
H_2O	Conventional	SO_2	Conventional
CO_2	Conventional	SO_3	Conventional
CO	Conventional	Cl_2	Conventional
H_2	Conventional	H_2S	Conventional

The process flow sheet in Aspen Plus® used for this model is shown in Figure 4.1. As no standard model in Aspen Plus® can alone describe the cyclone gasifier, a set of different blocks were used in the simulation. For all blocks in this simulation, a pressure of 0.65 barg was specified. The following assumptions were made in this model:

- Steady-state and isothermal process
- Instant drying and pyrolysis of biomass
- Equilibrium is reached and calculated by minimizing Gibbs free energy
- Perfect mixing giving uniform composition, temperature, and pressure
- Pressure drops are neglected
- Constant heat loss regardless of operating conditions
- No catalytic effects are considered
- Fuel handling system not considered; fuel is assumed to be grinded
- Char is represented as solid carbon (C) and inert ash separately
- No change in PSD during reaction is assumed
- All light non-aromatic compounds are defined by CH_4, C_2H_2 and C_2H_4
- Tars defined by benzene C_6H_6
- Nitrogen compounds defined as N_2, NO and NO_2

- Sulfur compounds defined as elemental S, SO_2, SO_3 and H_2S
- Chlorine compounds defined as Cl_2
- Minor by-products are neglected

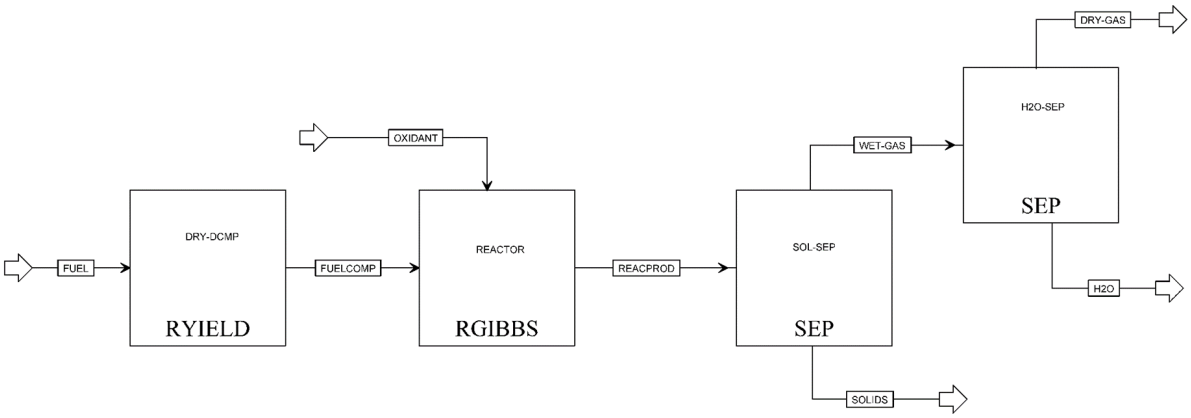

Figure 4.1. Process flow sheet for the equilibrium-based gasification model in Aspen Plus®.

The FUEL stream is specified at 30 °C and 1 atm with component attribute and PSD of ground virgin wood pellets according to Table 4.2 and Table 4.3, respectively. These analyses were done on wood pellets from a mixture of *Pinus sylvestris* and *Picea abies* used in this plant [2, 3].

Table 4.2. Proximate, ultimate and sulfanal analysis of virgin wood pellets used as fuel.

Element	**Value**
Proximate Analysis (wt.% on db, except moisture on wb)	
Moisture	6.2
Fixed carbon (FC)	9.55
Volatile matter (VM)	89.95
Ash	0.5
Ultimate Analysis (wt.% on db)	
Ash	0.5
Carbon (C)	51.4
Hydrogen (H)	6.3
Nitrogen (N)	0.05

Element	Value
Ultimate Analysis (wt.% on db)	
Chlorine (Cl)	0
Sulfur (S)	0.05
Oxygen (O)	41.7
Sulfanal analysis (wt.% on db)	
PYRITIC	0.023
SULFATE	0.004
ORGANIC	0.023

Table 4.3. PSD analysis of virgin wood pellets used as fuel.

Lower limit (µm)	Upper limit (µm)	Weight fraction
0	75	0.018
75	125	0.034
125	250	0.101
250	500	0.265
500	1000	0.490
1000	2000	0.092

Using the component attribute given in Table 4.2, a calculator block was used to specify mass yields of the first reactor block DRY-DCMP of type RYIELD. This calculator block uses the component analysis to achieve a mass balance when converting nonconventional component BIOMASS to conventional components and nonconventional component ASH. For simplicity, all fuel-bound N, S, and Cl are assumed to form N_2, elemental S and Cl_2 respectively. All moisture content in the biomass is assumed to be released as water vapor.

For the REACTOR block of type RGIBBS, calculation option was set to calculate phase equilibrium and chemical equilibrium as default with considering all components as possible products. A design specification was assigned to this simulation to calculate the correct temperature which closes the heat balance. The temperature was varied until the net heat duty from both reactor blocks equals to the heat loss of 80 kW measured in the plant [2].

Furthermore, a last calculator block was assigned to the OXIDANT stream to achieve the desired lambda value specified. The OXIDANT stream in the base case consisted of air with 101 °C and 0.65 barg.

Lastly, the two separation units SOL-SEP and H2O-SEP were of the block type SEP. These are assumed to ideally separate all solids and water, respectively, giving a dry product gas with no particles. Note that no cyclone model was specified to simulate behavior of particle separation in this simulation; this will instead be discussed in Section 4.3.

4.2 Combined equilibrium-based and kinetic-based gasification model with pyrolysis correlations

The components defined in this model are shown in Table 4.4. The same property methods and stream class were used as the model presented in Section 4.1.

Table 4.4. Components defined for the kinetic-based gasification model in Aspen Plus®.

Component	Type	Component	Type
BIOMASS	Nonconventional	CO_2	Conventional
ASH	Nonconventional	CO	Conventional
C	Solid	H_2	Conventional
S	Conventional	CH_4	Conventional
N_2	Conventional	C_2H_4	Conventional
O_2	Conventional	C_6H_6	Conventional
H_2O	Conventional	Cl_2	Conventional

The process flow sheet for the kinetic-based gasification model is shown in Figure 4.2. As no standard model in Aspen Plus® can alone describe the cyclone gasifier, a set of different blocks were used together in the simulation. For all blocks in this simulation, a pressure of 0.65 barg was specified. The following assumptions were made in this model:

- Steady-state and isothermal process
- Instant drying and pyrolysis of biomass
- Kinetic reaction rate expressions are used for all homogeneous reactions
- Equilibrium is calculated by minimizing Gibbs free energy for all heterogeneous reactions with temperature restriction approach
- Perfect mixing giving uniform composition, temperature, and pressure
- Pressure drops are neglected
- Constant heat loss regardless operating conditions
- No catalytic effects are considered

- Fuel handling system not considered, fuel is assumed to be ground
- Char is represented as solid carbon (C) and inert ash separately
- No change in PSD during reaction is simulated
- All light non-aromatic compounds are defined by CH_4 and C_2H_4 only
- Tars defined by benzene C_6H_6 only
- Nitrogen compound defined is only N_2
- Sulfur compound defined is only elemental S
- Chlorine compound defined is only Cl_2
- Minor by-products other than tars (benzene) are neglected

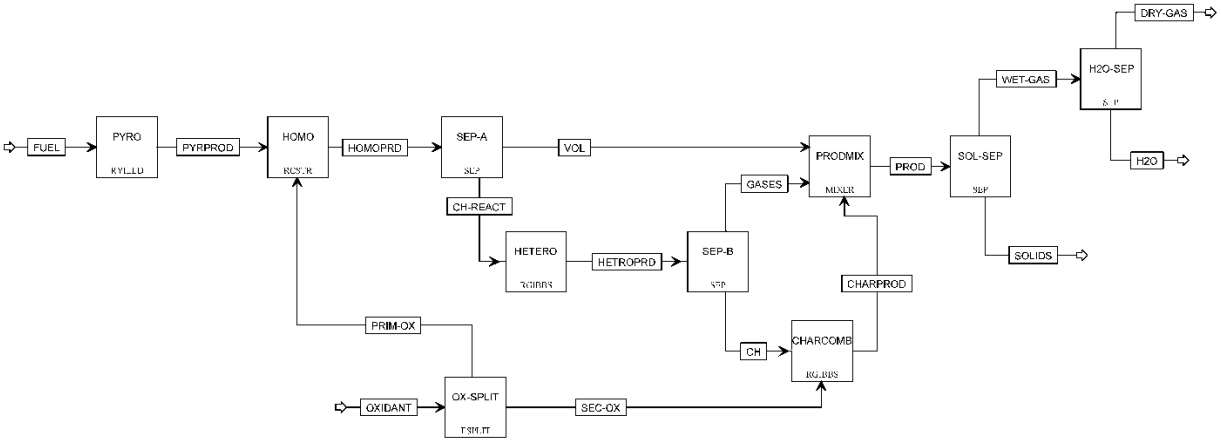

Figure 4.2. Process flow sheet for the kinetic-based gasification model in Aspen Plus®.

Fewer components are defined in this model in comparison with the equilibrium model presented in section 4.1. This is due to lack of kinetic expressions for all components defined in the first model. The FUEL stream is specified at 30 °C and 1 atm with the same Component Attribute and PSD as the model presented in Section 4.1. Using the Component Attribute given in Table 4.2, a calculator block was used to specify the mass yields of the first reactor block PYRO of type RYIELD. This calculator block uses correlations of pyrolysis product yields found in the literature in a FORTRAN code with temperature given in °C and fuel component analysis as input [4, 33].

The yield of tar on dry ash-free basis (daf) is given by the following equation, where tar is assumed to be only benzene [33]:

$$y_{tar,F} = (2.92 \times 10^{-2} - 2.0 \times 10^{-5}\, T)/(1 - y_{ash,F}) \quad (3)$$

The yields of H_2, CO, CH_4 and char are all obtained from another study and are given on daf basis [4]:

$$y_{H_2,F} = 1.145\left(1 - e^{-0.11\times10^{-2}T}\right)^{9.384} \quad (4)$$

$$y_{CO,F} = y_{H_2,F}\left(3 \times 10^{-4} + \frac{0.0429}{1+(T/632)^{-7.23}}\right)^{-1} \quad (5)$$

$$y_{CH_4,F} = -2.18 \times 10^{-4} + 0.146\, y_{CO,F} \quad (6)$$

$$y_{char,F} = 0.106 + 2.43\, e^{-0.66\times10^{-2}T} \quad (7)$$

The remaining yields of CO_2, H_2O and light non-aromatic hydrocarbons C_2H_4 are calculated by elemental mass balance of C, H and O according to [4]:

$$y_{C,F} - y_{ch,F} - y_{C,tar}y_{tar,F} = y_{C,C_2H_4}y_{C_2H_4,F} + y_{C,CH_4}y_{CH_4,F} + y_{C,CO}y_{CO,F} + y_{C,CO_2}y_{CO_2,F} \quad (8)$$

$$y_{O,F} = y_{O,CO}y_{CO,F} + y_{O,CO_2}y_{CO_2,F} + y_{O,H_2O}y_{H_2O,F} \quad (9)$$

$$y_{H,F} - y_{H,tar}\, y_{tar,F} = y_{H,C_2H_4}y_{C_2H_4,F} + y_{H,CH_4}y_{CH_4,F} + y_{H,H_2O}y_{H_2O,F} + y_{H_2,F} \quad (10)$$

These correlations are valid up to 1000 °C, therefore any temperature input above this value will be set to 1000 °C to avoid errors in mass balance. The yield of H_2O calculated with these correlations are excluding the moisture content of the fuel itself. Therefore, the total mass yield of water in the PYRO block is the sum of moisture content of the fuel and the calculated yield above. All fuel N, S and Cl are assumed to form N_2, elemental S and Cl_2 respectively.

The next reactor block is HOMO of type RCSTR with specified reactor volume of 0.98 m^3 [2]. This block contains the homogenous reactions with Arrhenius expressions according to Table 4.5 and activation energies in (kJ/kmol) [3]. The reacting phase for all reactions is chosen to vapor, rate basis to reactor volume, and concentration basis to molarity giving a reactant reaction rate in (kmol/m^3·s).

Table 4.5. Reactions specified in HOMO block with Arrhenius expressions.

No.	Reaction	Arrhenius expression (kmol/m^3·s)
1	$CH_4 + 1.5\ O_2 \rightarrow CO + 2\ H_2O$	$1.59\times10^{10}e^{-(\frac{200002}{RT})}[CH_4]^{0.7}[O_2]^{0.8}$
2	$CH_4 + H_2O \rightarrow CO + 3\ H_2$	$3\times10^{5}e^{-(\frac{125525}{RT})}[CH_4][H_2O]$
3	$C_2H_4 + 2\ O_2 \rightarrow 2\ CO + 2\ H_2O$	$1\times10^{12}e^{-(\frac{173297}{RT})}[C_2H_4][O_2]$
4	$H_2 + 0.5\ O_2 \rightarrow H_2O$	$1.8\times10^{10}e^{-(\frac{146401}{RT})}[H_2]^{1.5}[O_2]$
5	$CO + 0.5\ O_2 \rightarrow CO_2$	$1.24\times10^{10}e^{-(\frac{170304}{RT})}[CO][O_2]^{0.5}[H_2O]^{0.5}$
6	$CO + H_2O \rightarrow CO_2 + H_2$	$2.78e^{-(\frac{12560}{RT})}\left([CO][H_2O] - \frac{[CO_2][H_2]}{0.0265e^{(\frac{3958.5}{T})}}\right)$
7	$C_6H_6 + 4.5\ O_2 \rightarrow 6\ CO + 3\ H_2O$	$7.59\times10^{6}e^{-(\frac{201199}{RT})}[C_6H_6]^{-0.1}[O_2]^{1.85}$
8	$C_6H_6 + 6\ H_2O \rightarrow 6\ CO + 9\ H_2$	$3.0\times10^{5}e^{-(\frac{125525}{RT})}[C_6H_6][H_2O]$

In the next block SEP-A, all O_2, H_2O, CO_2, and solids are separated. These are allowed to react in HETERO block of type RGIBBS to consider the heterogeneous reactions 9–11 shown in Table 2.1. Arrhenius expressions for heterogeneous reactions were available in literature, however, these are not available for use directly in Aspen Plus®. An attempt was made to convert these to a form supported in Aspen Plus® without using FORTRAN or advanced equation-modeling without success. To be able to describe kinetics of char reactions, some consideration should be taken to the mass-transfer processes in the char particles.

The calculation option in HETERO was set to restrict chemical equilibrium by specifying the temperature approach with all components as possible products. A design specification was set to achieve the correct conversion of solid C compared to experimental data by varying the temperature approach. The temperature approach restriction in this block was set to -439 °C by this design specification, which means that equilibrium calculations are done at 439 °C below the specified block temperature.

Another block SEP-B was used to separate the unreacted solid C and ash from the products. These are allowed to react with the secondary air stream SEC-OX in CHARCOMB block of type RGIBBS, simulating the bottom of the gasifier. The calculation option was set to calculate phase equilibrium and chemical equilibrium as default with considering all components as possible products. No restriction of chemical equilibrium was set in this block. This is since solid char has a residence time of several minutes in the bottom of the real gasifier, in comparison with the residence time of few seconds of the gas-phase.

A design specification was assigned to this simulation to calculate the correct temperature which closes the heat balance. The temperature was varied until the net heat duty from all reactor blocks equals to the heat loss of 80 kW measured in the plant [2].

As all blocks are assumed to represent the gasifier, a calculator block is used to set the same temperature in all reactor blocks PYRO, HOMO, HETERO and CHARCOMB. Furthermore, a last calculator block was assigned to the OXIDANT stream to achieve the desired lambda value specified. The OXIDANT stream in the base case consists of air with 101 °C and 0.65 barg, this stream is divided in OX-SPLIT to obtain a smaller secondary air stream SEC-OX [2]. The two separation units SOL-SEP and H2O-SEP have the same function and input as specified for the model in Section 4.1.

4.3 Modification of gasifier models for adaptation to biological methanation

A slightly different approach is needed when studying the adaption of operating conditions to the subsequent biological methanation process. This is since a change in the gasifying medium from O_2/N_2 (air) to O_2/CO_2 will most probably affect the separation efficiency of the cyclone gasifier. This is because inlet velocity, volumetric flow rate and physical properties of the gasifying medium will change significantly. Another limitation is the gasification temperature. As mentioned in Section 2.3, the ash melting temperature will limit how high the temperature is allowed to be. For biomass defined in Table 4.2, the gasifier is operated at temperature of maximum 1000 °C at the top and 1200 °C at the bottom of the gasifier [2].

This approach is more difficult as no reactions can be defined in a cyclone gasifier without the use of advanced modeling with FORTRAN in Aspen Plus®. Therefore, a block REAC-CYC of type CYCLONE was added after the gasifier models developed in Sections 4.1 and 4.2. The cyclone was specified with dimensions as the real cyclone gasifier and default input of Muschelknautz as calculation method. However, only one inlet can be specified in Aspen Plus® as compared to two inlets found in the real gasifier.

Another limitation of the models is the neglect of change in PSD during reaction in the gasifier. To study the change of cyclone collection efficiency, an additional stream PARTICLE was added to the cyclone in Aspen Plus®. This stream has the same temperature and pressure as the PROD flow from the gasifier. Furthermore, 9.05 kg/h ash was assumed with a PSD as in Table 4.6 according to provided analysis [2].

Table 4.6. Assumed PSD analysis of produced ash in the cyclone gasifier.

Lower limit (µm)	Upper limit (µm)	Weight fraction	Lower limit (µm)	Upper limit (µm)	Weight fraction
0	0.018	0	0.36	0.578	0.1399
0.018	0.035	0.0107	0.578	0.946	0.0619
0.035	0.051	0.0470	0.946	1.512	0.0221
0.051	0.087	0.1343	1.512	2.4	0.0117
0.087	0.146	0.2106	2.4	4.024	0.0051
0.146	0.232	0.1857	4.024	6.35	0.0028
0.232	0.36	0.1605	6.35	19.671	0.0077

A calculator block was specified, which calculates the required flow of pure O_2 with specified lambda value as input. The same calculator block calculates the required flow of CO_2 to reach a specified molar fraction of CO_2 in the oxidant stream. It is important to note that the models do not implement a recirculation stream of CO_2 to prevent convergence problems in Aspen Plus® and make calculations faster. Another calculator block uses equations specified in Section 4 to calculate LHV of gas and CGE of process.

Finally, different lambda values and molar fractions of CO_2 was used in a sensitivity analysis to study the effect on temperature, carbon conversion, gas composition, tar mass flow, LHV of gas, CGE of process, residence time in reactor, pressure drop in cyclone and its particle collection efficiency. A comprehensive optimization study was not considered in this study, however, an initial design is proposed by considering some key parameters.

The main parameters considered are cyclone separation efficiency, gasifier temperature, the LHV of syngas and the CGE of the process. The main goal is to keep CGE as high as possible without significant drop in cyclone separation efficiency, and without reaching too high temperatures causing ash melt. Another goal is to keep a low CO_2 content as it requires separation from the product gas after the subsequent biological methanation. High CO_2 content will also cause lower LHV of the syngas [8].

In addition to the parameters mentioned above, the adaption should also consider CH_4 content and contaminants in the syngas as mentioned in Section 2.3. If different operating conditions results in similar LHV and CGE, then the case with higher CH_4 content and lower tar content should be chosen.

4.4 Gas-cleaning system model

The components defined in the gas-cleaning model are shown in Table 4.7, these components are present in the syngas entering the gas-cleaning system according to analysis [2].

For calculations of physical properties, the global property method chosen is non-random two-liquid (NRTL) according to the Aspen Plus® methods assistant. This method is an activity coefficient-based model which takes the non-ideality in the liquid phase into consideration. This non-ideality will most probably show in this process due to presence of tars in the water-based gas-cleaning system. Moreover, a literature review was conducted and some studies with tars involved in Aspen Plus® uses NRTL as the property method [34-39]. The used stream class was set to MCINCPSD as conventional and nonconventional solids were used with a defined PSD.

Table 4.7. Components defined for the gas-cleaning model in Aspen Plus®.

Component	Type	Component	Type
Ash	Nonconventional	Indene	Conventional
N_2	Conventional	Naphthalene	Conventional
H_2O	Conventional	2-Methylnaphthalene	Conventional
CO	Conventional	1-Methylnaphthalene	Conventional
CO_2	Conventional	Diphenyl	Conventional
H_2O	Conventional	Acenaphthylene	Conventional
CH_4	Conventional	Acenaphthene	Conventional
C_2H_2	Conventional	Fluorene	Conventional
C_2H_4	Conventional	Phenanthrene	Conventional
C_2H_6	Conventional	Anthracene	Conventional

Component	Type	Component	Type
Benzene	Conventional	Fluoranthene	Conventional
Toluene	Conventional	Pyrene	Conventional
m-Xylene	Conventional	Phenol	Conventional
o-Xylene	Conventional	*o*-Cresol	Conventional
Indane	Conventional	*p*-Cresol	Conventional

The process flow sheet in Aspen Plus® used for this model is shown in Figure 4.3. As no standard model in Aspen Plus® can alone describe all operating units, a set of different blocks were used together in the simulation. The following assumptions were made in this model:

- Steady-state and isothermal process
- Perfect mixing giving uniform composition, temperature, and pressure within all blocks except where RADFRAC (the distillation model) is used
- No heat losses are considered due to lack of measurements
- No reactions within the blocks are considered
- Ash is inert, it does not interact with tars or other components
- Nitrogen compound defined is only N_2
- Sulfur compound defined is only elemental S
- Chlorine compound defined is only Cl_2
- Minor by-products other than tars are neglected
- Some separation units such as FLASH2 and RADFRAC are assumed to have a constant separation efficiency despite of operating conditions. This is due to limitation of Aspen Plus® standard block models.

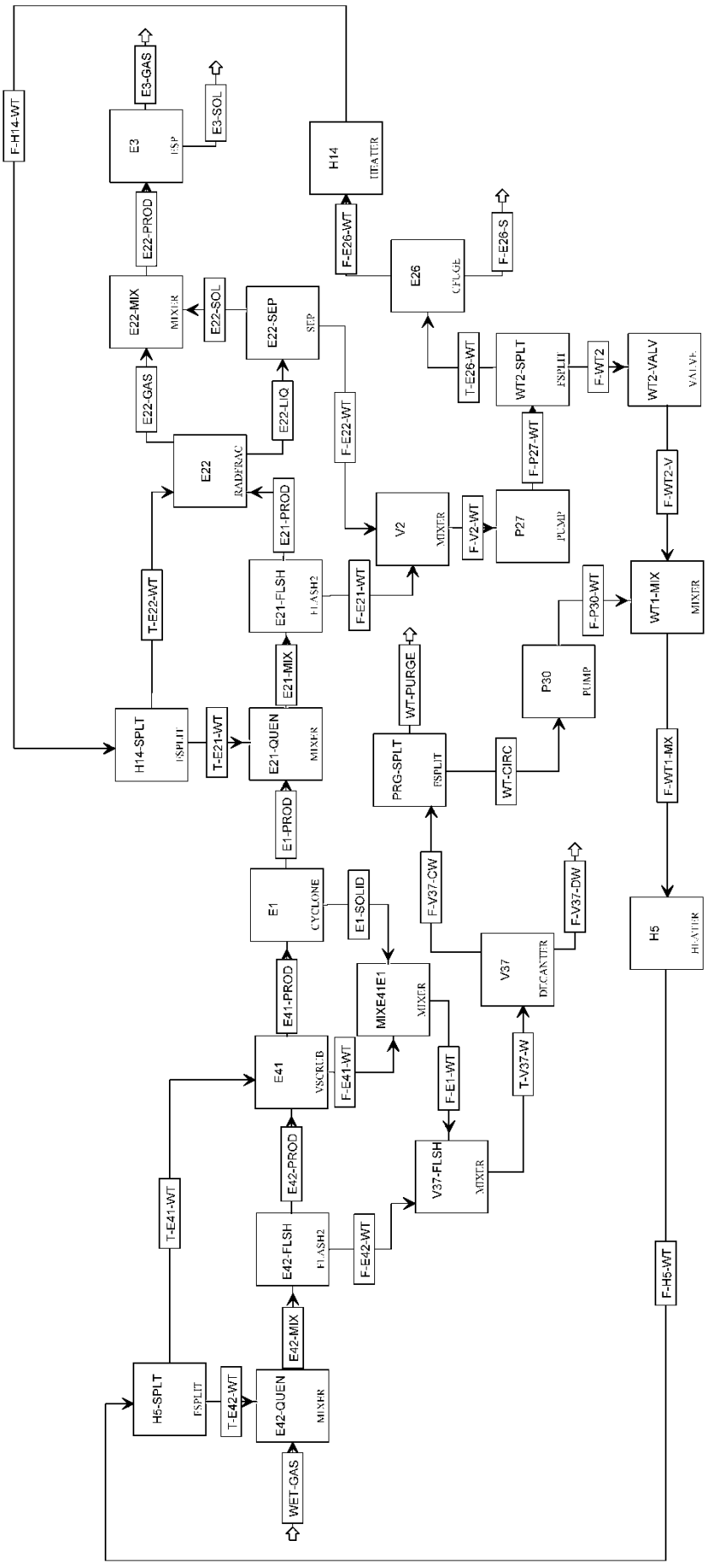

Figure 4.3. Process flow sheet for the gas-cleaning model in Aspen Plus®.

It is worth noting that the gasifier simulation and the gas-cleaning simulation are not connected in Aspen Plus®, which could be done by creating different hierarchies in the same file. This was initially done but was removed afterwards to minimize computation time. The specification of the WET-GAS stream is done with input from experimental data from the base case. Here, ash is assumed following the same PSD as presented in Table 4.6.

When the gasifier product stream WET-GAS enters the first block E42-QUEN of type MIXER, water through stream T-E42-WT is added to cool the gas. The block E42-QUEN together with the FLASH2 block E42-FLSH are used to simulate the first quench unit. A pressure drop of -53.1 mbar is assumed here with particle separation efficiency of 60% according to experimental data [2].

The gas stream E42-PROD enters a VSCRUB block E41 simulating the venturi scrubber with water in stream T-E41-WT used to separate solids and cool the gas. The calculation method used in E41 is set to Calvert with a round throat of a diameter determined by a design specification. This design specification varies the diameter of the venturi scrubber until 100 mbar in pressure drop is reached across it.

The gas stream E41-PROD then enters a cyclone E1 which is specified with dimensions as the real cyclone and default input of Leith-Licht as calculation method. After this stage, all contaminated cooling water from all blocks above are mixed and flashed into atmospheric pressure in V37-FLSH.

A DECANTER model named V37 is used to simulate the sedimentation tank that is used to provide clean cooling water. The sedimentation tank is operating at atmospheric pressure with same temperature as inlet stream T-V37-W, therefore, a calculator block was used to set the temperature. In this block, the property method used is PR-BM as using NRTL resulted in no phase separation in the DECANTER. A splitter PRG-SPLT is used to purge excess water produced in the process. The split fraction in PRG-SPLIT is specified using a design specification, which varies the fraction so that a constant amount of water is maintained in the first water cycle. A cooler H5 and pump P30 are used to cool and increase the pressure of recirculated water to 54 °C and 3.3 barg respectively.

The second water quench is simulated similarly to the first quench by using blocks E21-QUEN and E21-FLSH. No pressure drop is assumed here, a particle separation efficiency is set to 30% according to experimental data [2]. A packed column scrubber E22 is simulated using a RADFRAC block. The calculation type is set to rate-Based with 10 stages, neither condenser nor evaporator are used. The top of column is set to have a pressure of 0.345 barg according to experimental data with gas stream E21-PROD specified On-Stage. The column packing is defined by one section covering all stages, with section diameter 0.6 m and 3 m in height. The packing material used is INTALOX-A by KOCH, which is made of metal and have 40-MM in dimension according to product specification. A SEP block named E22-SEP is added after the column. This separation block is used to achieve the correct particle separation efficiency of the column, which is about 80%.

The process water from the second water quench and the packed scrubber are mixed in the second water cycle by the V2 block. The water is pumped to 5.8 barg with some water split in WT2-SPLT. The split fraction is calculated with a design specification, where it is varied until a gas temperature of 40 °C is reached after the packed scrubber. The water not split is led through a centrifuge E26 simulated with CFUGE, a Decanter model type is used with *Ideal*

separation and specified residual moisture of 0.75 on wet-basis. Before recirculating cooling water to the second water cycle, a cooler H14 is used to cool it to 36 °C with pressure decreased to 4.6 barg.

Finally, the product gas E22-PROD is led through a block E3 of type ESP simulating the WESP with a pressure drop of about 45 mbar. A tubular model is used with Deutsch as calculation method, the fitting parameter exponent K is set to 8 to achieve separation according to experimental data. The tube radius is set to 125 mm, length to 2992 mm and spray electrode radius to 5 mm with 31 tubes. The WESP is set to have a voltage of 40 kV, all according to product specification of the WESP.

5 Results and discussion

5.1 Validation of equilibrium-based gasification model

The equilibrium-based gasification model presented in Section 4.1 was validated against experimental data from the plant. Figure 5.1 shows the gas yields of produced syngas when 773 kg/h virgin wood pellets were gasified at 0.65 barg with 1103 kg/h primary air flow and 45 kg/h secondary air flow. Main components are presented as mol component per a unit of dry ash-free fuel (mol/$kg_{F,daf}$).

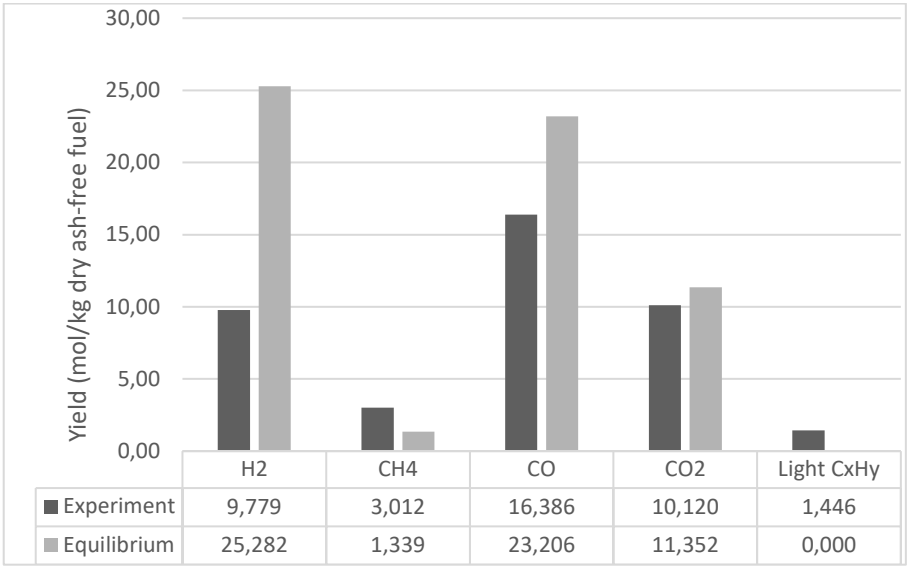

	H2	CH4	CO	CO2	Light CxHy
Experiment	9,779	3,012	16,386	10,120	1,446
Equilibrium	25,282	1,339	23,206	11,352	0,000

Figure 5.1. Gas yields of dry syngas (mol/$kg_{F,daf}$) when 773 kg/h biomass was gasified with 1103 kg/h primary air flow and 45 kg/h secondary air flow. Equilibrium-based model in light grey and experimental data in dark grey.

It was found from experimental data that the wet syngas has 9.0 vol.% water with 1356 Nm^3/h in gas flow, LHV of 5.94 MJ/Nm^3 and 13 kg/h tars. The average reactor temperature was about 881 °C with a CGE of 0.60 [2]. The equilibrium-based model shows a wet syngas with 6.4 vol.% water, 1848 Nm^3/h in gas flow, LHV of 5.35 MJ/Nm^3 and 0 kg/h tars. The calculated reactor temperature was 687 °C with a CGE of 0.70.

As observed, the reactor temperature is much lower when equilibrium is assumed. This behavior was expected as the model assumes infinite residence time for components in the defined system until equilibrium is reached. However, process data shows a residence time of few seconds in the real gasifier. The process does not reach equilibrium due to the relevant low temperature and short residence time, which results in incomplete fuel conversion. When converting the fuel, there are mainly two endothermic reactions lowering reactor temperature, these are shown in Table 2.1 as reactions 10 and 11. As less char reacts in the real gasifier, less energy is consumed by the system making the real temperature higher.

There is also a large deviation in yields of gases between the model and experimental data. The model underestimates yield of CH_4 and light non-aromatic hydrocarbons but overesti-

mates H_2 and CO. This is a common behavior observed in other equilibrium models found in previous studies, as these models are based on minimization of Gibbs free energy until equilibrium is reached [14, 16, 19, 21].

The effect of gas temperature was studied in the real gasifier by varying the mass flow of air with experimental data available. Figure 5.2 shows the measured gas yields of produced syngas, with temperature in °C shown in the plot legend. As seen, the temperature increases due to increasing flow of air which allows higher conversion of fuel. Main components are presented as mol component per a unit of dry ash-free fuel (mol/$kg_{F,daf}$).

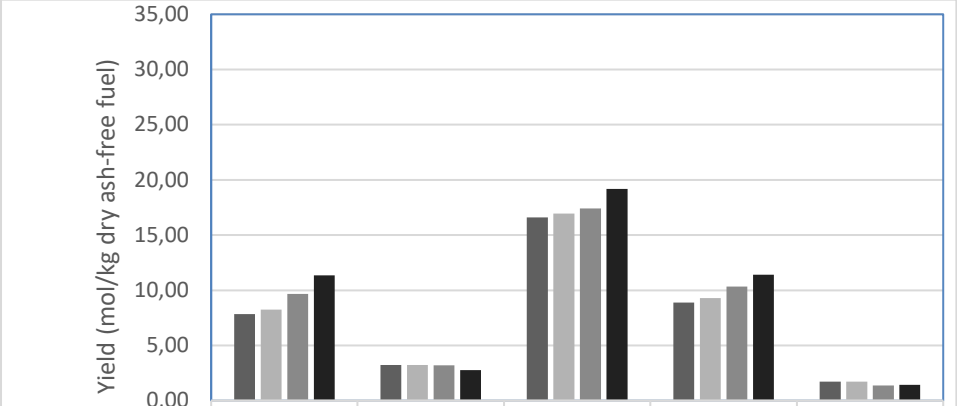

	H2	CH4	CO	CO2	Light CxHy
EXP1 (859 °C)	7,839	3,228	16,599	8,876	1,729
EXP2 (904 °C)	8,242	3,228	16,945	9,280	1,729
EXP3 (950 °C)	9,668	3,202	17,402	10,332	1,389
EXP4 (1003 °C)	11,354	2,767	19,193	11,412	1,441

Figure 5.2. Measured gas yields of produced syngas (mol/$kg_{F,daf}$) with gas temperature in °C for different cases.

The same input was used in the equilibrium-based model to study the variation of yields with temperature. Figure 5.3 shows the predicted equilibrium gas yields of produced syngas (mol/$kg_{F,daf}$) with reactor temperature in °C shown in the plot legend. Unfortunately, deviation in yield of all components is observed here also with same reasons as mentioned previously. However, the trend of all components follows experimental data except for CO_2 and light non-aromatic hydrocarbons.

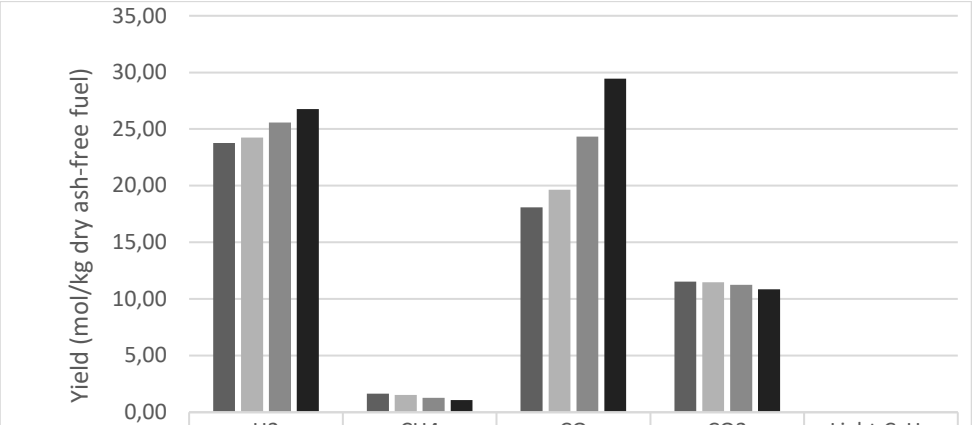

	H2	CH4	CO	CO2	Light CxHy
EQ1 (669 °C)	23,756	1,644	18,089	11,542	0,000
EQ2 (675 °C)	24,262	1,541	19,633	11,489	0,000
EQ3 (691 °C)	25,586	1,284	24,324	11,239	0,000
EQ4 (705 °C)	26,756	1,074	29,439	10,864	0,000

Figure 5.3. Predicted equilibrium gas yields of produced syngas (mol/kg$_{F,daf}$) with reactor temperature in °C for different cases.

5.2 Validation of combined equilibrium-based and kinetic-based gasification model

The combined equilibrium-based and kinetic-based gasification model presented in Section 4.2 is validated against experimental data from the plant. Figure 5.4 shows the gas yields of produced syngas when 773 kg/h biomass was gasified with 1103 kg/h primary air flow and 45 kg/h secondary air flow. Main components are presented as mol component per a unit of dry ash-free fuel (mol/kg$_{F,daf}$).

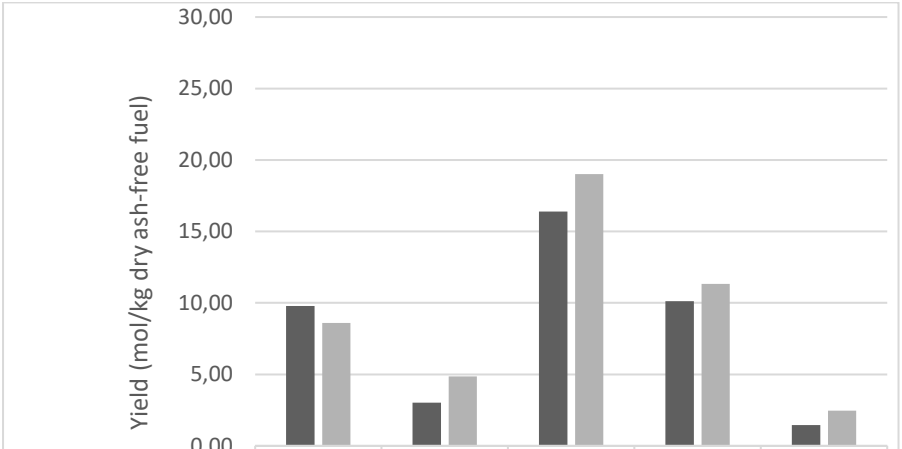

	H2	CH4	CO	CO2	Light CxHy
Experiment	9,779	3,012	16,386	10,120	1,446
Equilibrium/kinetic	8,604	4,858	19,003	11,321	2,462

Figure 5.4. Gas yields of dry syngas (mol/kg$_{F,daf}$) when 773 kg/h biomass was gasified with 1103 kg/h primary air flow and 45 kg/h secondary air flow. Equilibrium/kinetic based model in light grey and experimental data in dark grey.

The equilibrium/kinetic based model shows a wet syngas with 11.2 vol.% water with 1584 Nm^3/h in gas flow, LHV of 6.83 MJ/Nm^3 and 8.4 kg/h tars. The calculated reactor temperature was 878 °C with a CGE of 0.77.

Results from this model agrees with experimental data more than the equilibrium model, however, still some deviations are observed in gas yields. The deviation is most probably since heterogeneous reactions presented in Table 2.1 are simulated by assuming equilibrium. Furthermore, the two reactor blocks HOMO and HETERO are in series, which means that the homogenous reactions occur first, and then heterogeneous reactions occurs afterwards. However, in reality all reactions occur together in the real gasifier. The deviation in yield of light non-aromatic hydrocarbons is most probably due to these components being all lumped into C_2H_4 compared to C_2H_4, C_2H_6, and C_2H_2 measured in the real gasifier [2].

Results from all models are summarized in Table 5.1 and Figure 5.5 together with experimental data from the base case. As seen in the table, the CGE is higher for the models compared to experimental data. This deviation is due to the differences in temperature, tar flow rate, char conversion and product gas composition.

Table 5.1. Temperature, tar flow, LHV and CGE for all models and experimental data for the base case.

Variable	**Source**		
	Experimental data	**Equilibrium model**	**Kinetic model**
Temperature (°C)	881	687	878
Tar flow (kg/h)	13	0	8.43
LHV inc. tars (MJ/Nm^3)	5.94	5.35	6.83
CGE inc. tars (-)	0.60	0.70	0.77

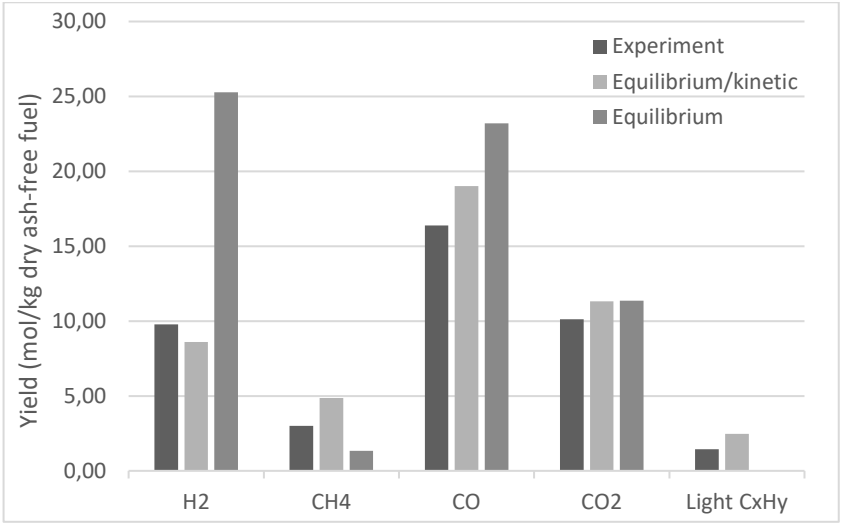

Figure 5.5. Gas yields of dry syngas ($mol/kg_{F,daf}$) for all models and experimental data for the base case.

Variation of gas yields with temperature was also studied for this model, with the same input as measurements shown in Figure 5.2. Figure 5.6 shows the predicted gas yields of produced syngas (mol/$kg_{F,daf}$) with gas temperature in °C shown in the plot legend. Note that the measured temperatures in Figure 5.2 are the gas temperature, compared to temperatures in Figure 5.3 and Figure 5.6 which can be interpreted as the average temperature in the gasifier [2]. Therefore, temperatures between Figure 5.2 and Figure 5.6 should be compared relative the trend of change between cases rather than comparison between absolute values.

As observed in Figure 5.6, the change in yields of H_2, CO and CO_2 follow the same trend observed in measurements. However, yields of CH_4 and light non-aromatic hydrocarbons show a deviation from this trend. This could be explained by the fact that the restriction with temperature approach in this model, as explained in Section 4.2, was made by using the design specification relative the base case. Moreover, all non-aromatic light hydrocarbons were lumped into C_2H_4 compared to C_2H_4, C_2H_6, and C_2H_2 measured in the real gasifier.

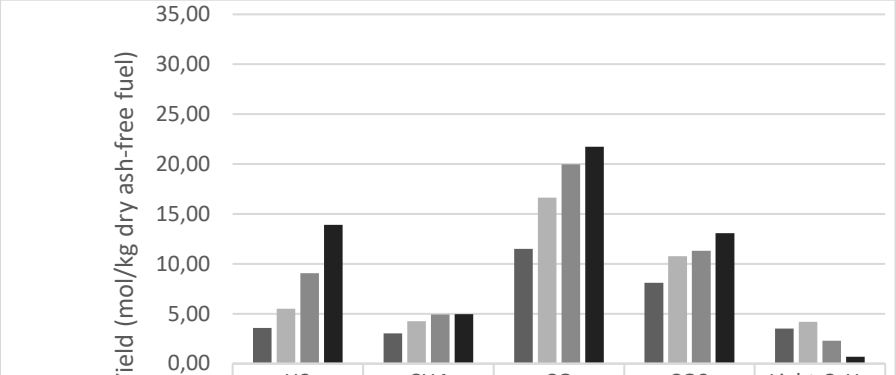

	H2	CH4	CO	CO2	Light CxHy
EQ/KIN1 (801 °C)	3,565	3,029	11,499	8,086	3,505
EQ/KIN2 (819 °C)	5,502	4,241	16,630	10,750	4,192
EQ/KIN3 (885 °C)	9,071	4,913	19,961	11,316	2,304
EQ/KIN4 (956 °C)	13,916	4,953	21,744	13,066	0,701

Figure 5.6. Predicted equilibrium/kinetic gas yields (mol/$kg_{F,daf}$) of produced syngas with reactor temperature in °C for different cases.

As experimental data was available on variation of fuel moisture, a validation of this effect was done for this model by varying fuel moisture and comparing to measurements [8]. This approach is done by either allowing drop of gasifier temperature or by increasing air flow to maintain the temperature [2].

Figure 5.7 shows the measured gas yields of produced syngas (mol/$kg_{F,daf}$) with fuel moisture content in wt.% shown in the plot legend. This was done without additional air which allowed temperature drop. The temperature dropped by increasing fuel moisture content, due to more energy needed to vaporize higher moisture content and more energy needed for the increased endothermic reaction with water. The temperature of the different cases EXP5 to EXP8 were 959, 953, 946 and 935 °C respectively [2].

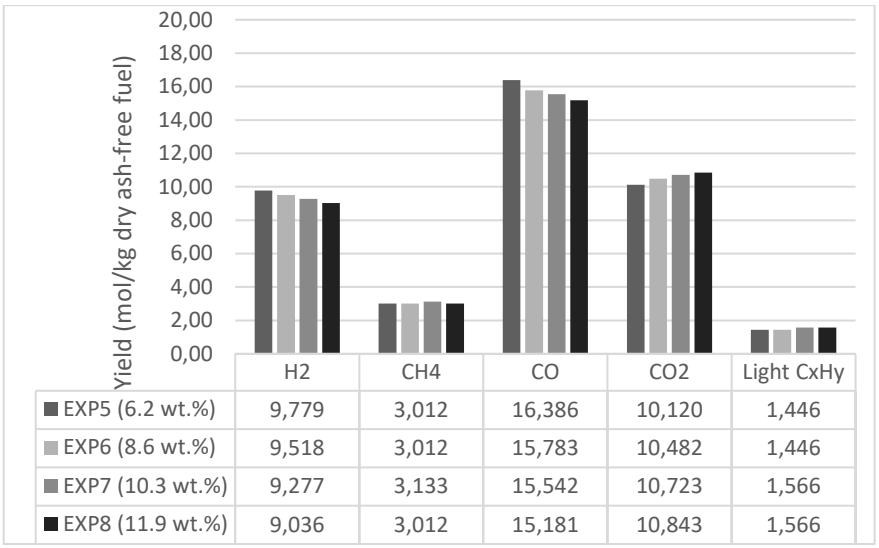

	H2	CH4	CO	CO2	Light CxHy
EXP5 (6.2 wt.%)	9,779	3,012	16,386	10,120	1,446
EXP6 (8.6 wt.%)	9,518	3,012	15,783	10,482	1,446
EXP7 (10.3 wt.%)	9,277	3,133	15,542	10,723	1,566
EXP8 (11.9 wt.%)	9,036	3,012	15,181	10,843	1,566

Figure 5.7. Measured gas yields of produced syngas (mol/kg$_{F,daf}$) with fuel moisture content in wt.% for different cases. This was done without additional air which allowed temperature drop reaching 959, 953, 946 and 935 °C respectively.

The same input was used in the equilibrium/kinetic model with results presented in Figure 5.8. This figure shows the predicted gas yields of produced syngas (mol/kg$_{F,daf}$) with fuel moisture content in wt.% shown in the plot legend. The temperature of the different cases EQ/KIN5 to EQ/KIN8 were 878, 872, 866 and 860 °C respectively.

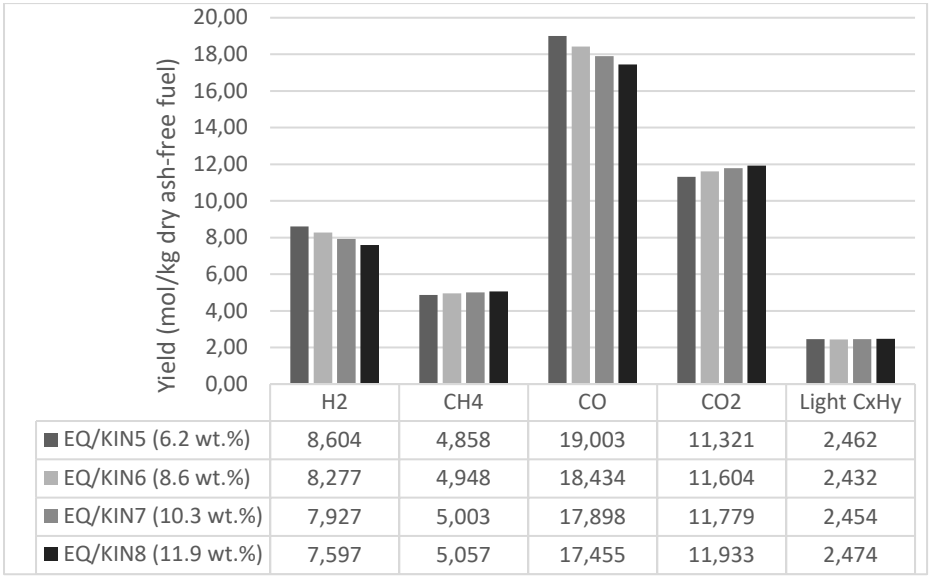

	H2	CH4	CO	CO2	Light CxHy
EQ/KIN5 (6.2 wt.%)	8,604	4,858	19,003	11,321	2,462
EQ/KIN6 (8.6 wt.%)	8,277	4,948	18,434	11,604	2,432
EQ/KIN7 (10.3 wt.%)	7,927	5,003	17,898	11,779	2,454
EQ/KIN8 (11.9 wt.%)	7,597	5,057	17,455	11,933	2,474

Figure 5.8. Predicted gas yields of produced syngas (mol/kg$_{F,daf}$) with fuel moisture content in wt.% for different cases. This was done without additional air which allowed temperature drop reaching 878, 872, 866 and 860 °C respectively.

Figure 5.9 shows the measured gas yields of produced syngas (mol/$kg_{F,daf}$) with fuel moisture content in wt.% shown in the plot legend. This was done with additional air which maintained the gasifier temperature by more conversion of fuel. It is observed that the yield of CO_2 increases significantly with moisture content but not H_2, which would be expected by the water-gas shift reaction. However, the increase of CO_2 in this case is most probably due to the increased fuel combustion, not due to water-gas shift reaction. The temperature of the different cases EXP9 to EXP12 were 950, 952, 951 and 953 °C respectively.

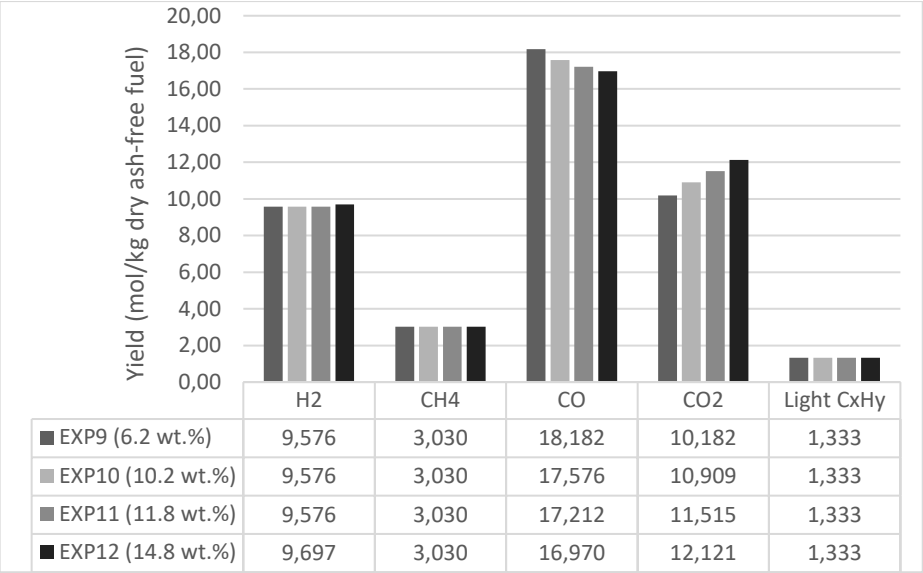

	H2	CH4	CO	CO2	Light CxHy
EXP9 (6.2 wt.%)	9,576	3,030	18,182	10,182	1,333
EXP10 (10.2 wt.%)	9,576	3,030	17,576	10,909	1,333
EXP11 (11.8 wt.%)	9,576	3,030	17,212	11,515	1,333
EXP12 (14.8 wt.%)	9,697	3,030	16,970	12,121	1,333

Figure 5.9. Measured gas yields of produced syngas (mol/$kg_{F,daf}$) with fuel moisture content in wt.% for different cases. This was done with additional air which maintained the gasifier temperature to 950, 952, 951 and 953 °C respectively.

The same input was used in the equilibrium/kinetic model with results presented in Figure 5.10. This figure shows the predicted gas yields of produced syngas (mol/$kg_{F,daf}$) with fuel moisture content in wt.% shown in the plot legend. The temperature of the different cases EQ/KIN9 to EQ/KIN12 were 883, 887, 910 and 893 °C respectively.

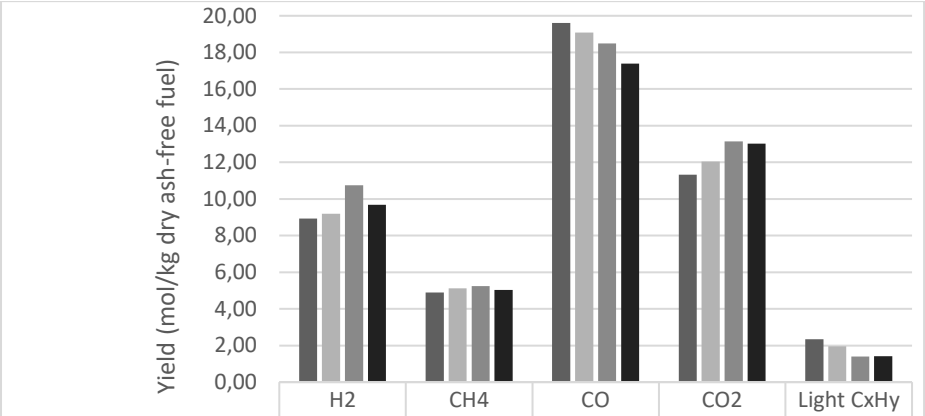

	H2	CH4	CO	CO2	Light CxHy
EQ/KIN9 (6.2 wt.%)	8,932	4,897	19,610	11,330	2,345
EQ/KIN10 (10.2 wt.%)	9,197	5,116	19,091	12,039	1,960
EQ/KIN11 (11.8 wt.%)	10,743	5,236	18,493	13,136	1,390
EQ/KIN12 (14.8 wt.%)	9,678	5,038	17,387	13,024	1,412

Figure 5.10. Predicted gas yields of produced syngas (mol/kg$_{F,daf}$) with fuel moisture content in wt.% for different cases. This was done with additional air which maintained the gasifier temperature to 883, 887, 910 and 893 °C respectively.

The model can predict trends for most components shown by experimental data as seen by comparing Figure 5.7 with Figure 5.8, and Figure 5.9 with Figure 5.10. The deviations observed could be explained by the fact that the restriction with temperature approach in this model, as explained in Section 4.2, was made by using the design specification relative the base case.

5.3 Validation of gas-cleaning system

When validating the gas-cleaning system, a gas stream was used with experimental data available. In this case, 1900 kg/h syngas at 959 °C and 0.65 barg was measured with composition as mass fraction presented in Table 5.2 [2].

Table 5.2. Mass fraction of components measured in syngas with 1900 kg/h at 959 °C and 0.65 barg used as input to the model.

Component	Mass fraction (-)	Component	Mass fraction (-)
Ash	0.0289	Indene	0.0005
N_2	0.4912	Naphthalene	0.0026
H_2O	0.0603	2-Methylnaphthalene	$5.241 \cdot 10^{-5}$
CO	0.1809	1-Methylnaphthalene	$3.990 \cdot 10^{-5}$
CO_2	0.1849	Diphenyl	$7.785 \cdot 10^{-5}$
H_2	0.0079	Acenaphthylene	0.0012
CH_4	0.0186	Acenaphthene	0.0001
C_2H_2	0.0047	Fluorene	0.0002
C_2H_4	0.0091	Phenanthrene	0.0007
C_2H_6	0.0001	Anthracene	0.0002
Benzene	0.0062	Fluoranthene	0.0004
Toluene	0.0004	Pyrene	0.0005
m-Xylene	$4.475 \cdot 10^{-5}$	Phenol	$6.583 \cdot 10^{-6}$
o-Xylene	0.0001	*o*-Cresol	$2.895 \cdot 10^{-6}$
Indane	0	*p*-Cresol	$1.328 \cdot 10^{-6}$

The output of the model was compared to experimental data on clean syngas available from the plant, the results are presented in Table 5.3 with concentrations in µg/ml [2].

Table 5.3. Concentration of components (µg/ml) from experimental measurements on clean syngas and predicted concentrations from gas-cleaning model.

Component	**Concentration (µg/ml)**		**Component**	**Concentration (µg/ml)**	
	Experimental	**Model**		**Experimental**	**Model**
Benzene	10.58	8.738	Acenaphthylene	0	~ 0
Toluene	0.9076	0.5771	Acenaphthene	0	~ 0
m-Xylene	0.0587	0.0631	Fluorene	0.0602	~ 0
o-Xylene	0.4142	0.2012	Phenanthrene	0	~ 0
Indane	0	0	Anthracene	0	~ 0
Indene	0.7842	~ 0	Fluoranthene	0	0
Naphthalene	1.334	~ 0	Pyrene	0.0390	0
2-Methylnaphthalene	0	~ 0	Phenol	No data	0.0048
1-Methylnaphthalene	0	0.0555	*o*-Cresol	No data	~ 0
Diphenyl	0	~ 0	*p*-Cresol	No data	0.0008

The highest error is found in separation of indene, naphthalene, 1-methylnaphthalene, Fluorene and Pyrene. Unfortunately, no data was available on concentrations of phenol, *o*-cresol, and *p*-cresol. There are many sources of error for these deviations, mainly the neglect of interaction between ash and soot particles with tars. Another major error source is the choice of physical property method. Comparison of different methods such as Peng Robinson cubic equation of state (PR) and Soave-Redlich-Kwong equation of state (RK-SOAVE) should be done in further studies. This was not done in this study due to time limitation.

The last-mentioned error source is most obvious when modeling the sedimentation tank V37 as a DECANTER in Aspen Plus®. Experimental data on suspension concentration in water after the sedimentation tank is available. These are compared to predicted values and presented in Table 5.4. Concentration of dirty water is given in g/L and clean water in mg/L. The deviations between experimental and predicted data are big and can be explained by the errors in separation of the different components as shown in Table 5.3.

Table 5.4. Experimental data on suspension concentration in water after sedimentation tank compared to predicted concentrations. All presented as concentration of dirty water in g/L and clean water in mg/L.

Component	Experimental	Model	Unit
Clean process water	1–2	82.13	mg/L
Dirty process water	10–50	153.4	g/L

5.4 Adaptation of gasification process to subsequent biological methanation

For the same fuel flow rate and components attribute as presented in Table 4.2, an exchange of O_2/N_2 (air) as gasifying medium to O_2/CO_2 was done. The aim was to obtain a similar temperature and cyclone particle separation efficiency as the (air) base case presented in Section 5.2 using the equilibrium/kinetic model.

Figure 5.11 shows the predicted gas yields of produced syngas when 773 kg/h biomass was gasified with same lambda value as the base case. The oxidation medium in this case is a mixture of 21 mol.% O_2 and 79 mol.% CO_2, giving a total oxidant flow rate of 1651 kg/h. Main components are presented as mol component per a unit of dry ash-free fuel (mol/$kg_{F,daf}$). The yield of CO_2 presented are excluding the recirculated molar flow rate of CO_2 in the gasifying medium.

This setup resulted in a syngas with 17.5 vol.% water, 1423 Nm^3/h in gas flow, LHV of 7.10 MJ/Nm^3 and 9.84 kg/h tars. The calculated reactor temperature was 781 °C with a CGE of 0.72. The pressure drop calculated is 183 mbar with a particle separation efficiency of 99.6%. The predicted gas composition on dry basis for this case is presented in Figure 5.11.

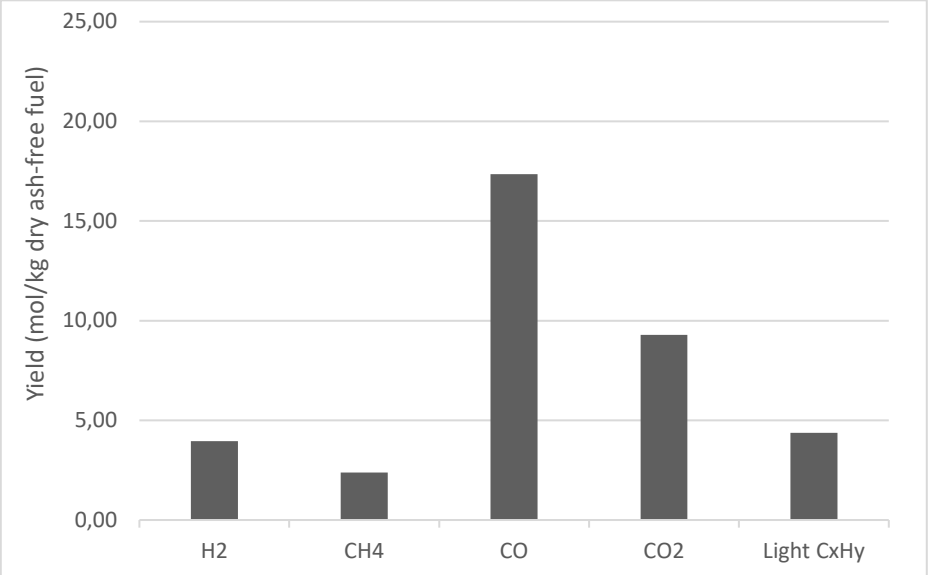

Figure 5.11. Predicted gas yields (mol/$kg_{F,daf}$) when 773 kg/h biomass was gasified with a 1651 kg/h oxidant mixture of 21 mol.% O_2 and 79 mol.% CO_2.

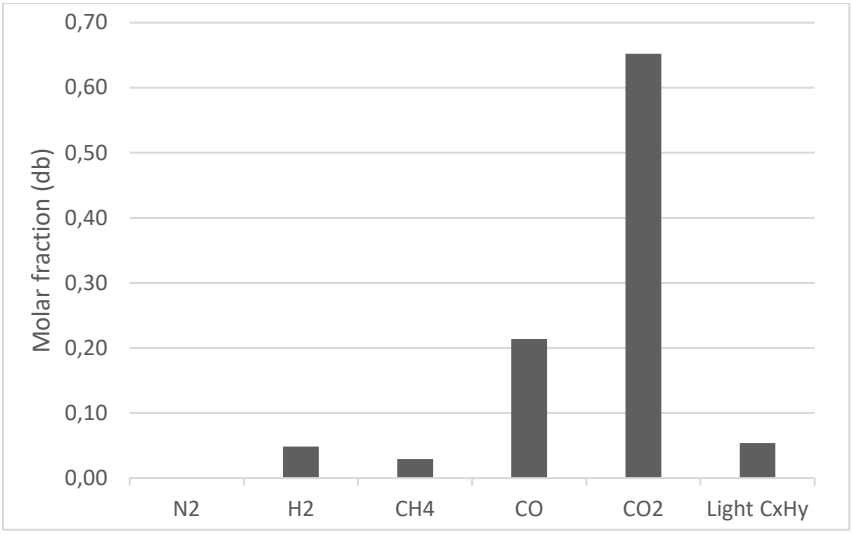

Figure 5.12. Predicted dry syngas molar composition when 773 kg/h biomass was gasified with a 1651 kg/h oxidant mixture of 21 mol.% O_2 and 79 mol.% CO_2.

Another approach is keeping the molar flow rate of O_2 as the base case and choosing the CO_2 flow rate to obtain similar total mass flow rate of oxidative stream. The gasifying medium in this case is a mixture of 29.5 mol.% O_2 and 70.5 mol.% CO_2. Main components are presented in Figure 5.13 as mol component per a unit of dry ash-free fuel (mol/$kg_{F,daf}$). The yield of CO_2 presented are excluding the recirculated molar flow rate of CO_2 in the gasifying medium.

This setup resulted in a gas with 17.1 vol.% water, 1247 Nm^3/h in gas flow, LHV of 8.34 MJ/Nm^3 and 8.70 kg/h tars. The calculated reactor temperature was 859 °C with a CGE of 0.74. The pressure drop calculated is 134 mbar with a particle separation efficiency of 99.6%. The predicted gas composition on dry basis for this case is presented in Figure 5.14.

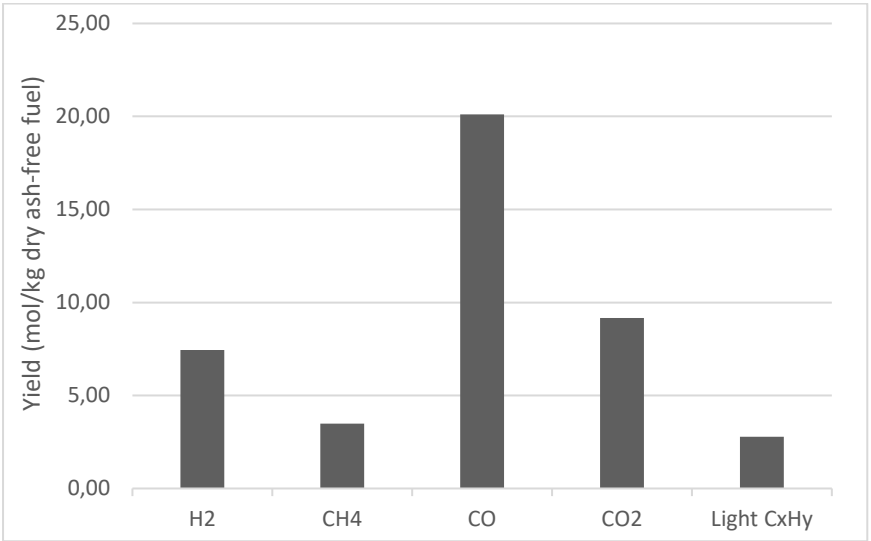

Figure 5.13. Predicted gas yields (mol/$kg_{F,daf}$) when 773 kg/h biomass was gasified with 1148 kg/h gasifying medium consisting of 29.5 mol.% O_2 and 70.5 mol.% CO_2.

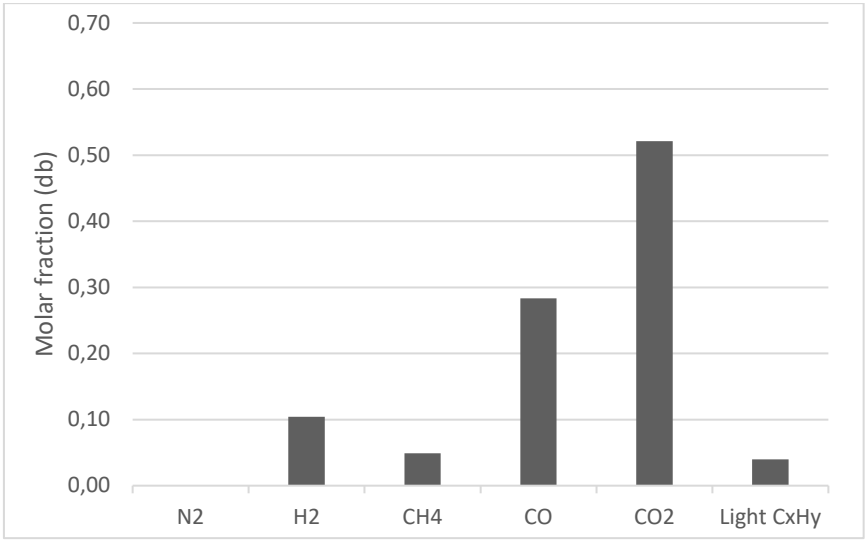

Figure 5.14. Predicted dry syngas molar composition when 773 kg/h biomass was gasified with 1148 kg/h gasifying medium consisting of 29.5 mol.% O_2 and 70.5 mol.% CO_2.

The results of all modeled cases are presented in Figure 5.15, Figure 5.16 and Table 5.5 for easier comparison. Moreover, LHV excluding tars are also calculated as it is more relevant for the biological methanation process. As seen, higher water content is predicted when O_2/CO_2 is used instead of air as gasifying medium. The reason behind this is maybe due to a change in the reaction rates of the heterogeneous reactions presented in Table 2.1, which might be confirmed by the decreased char conversion in Table 5.5.

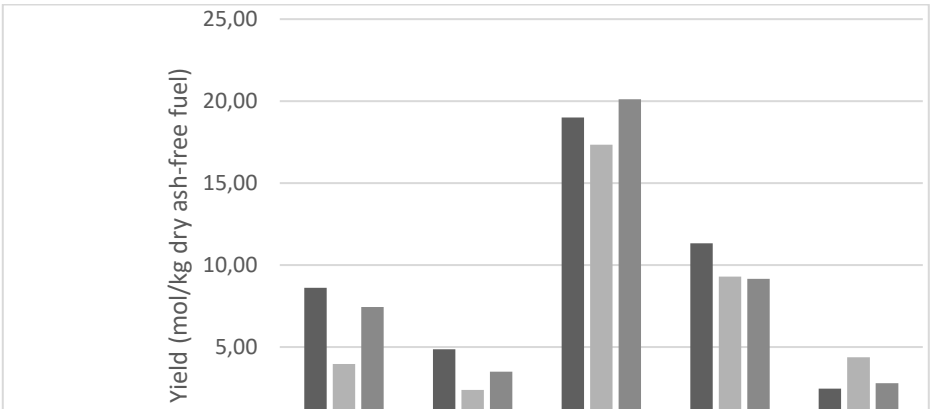

	H2	CH4	CO	CO2	Light CxHy
Base case	8,604	4,858	19,003	11,321	2,462
21% O2, 79% CO2	3,956	2,375	17,342	9,286	4,366
29.5% O2, 70.5% CO2	7,437	3,483	20,103	9,162	2,788

Figure 5.15. Predicted gas yields (mol/kg$_{F,daf}$) when 773 kg/h biomass was gasified for the different cases compared to the base case.

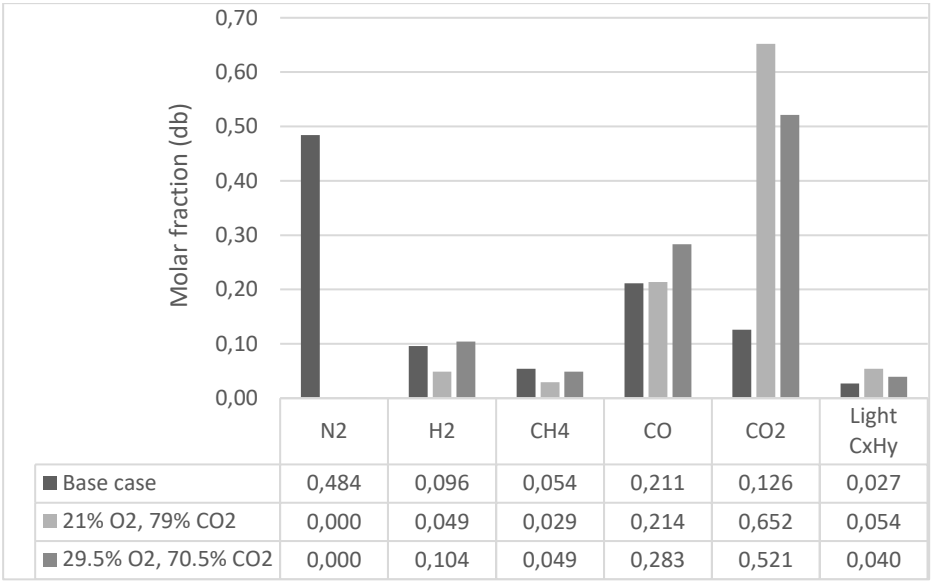

Figure 5.16. Predicted dry syngas molar composition when 773 kg/h biomass was gasified for the different cases compared to the base case.

Table 5.5. Temperature, flow rates, LHV, CGE, separation efficiency and gas water content for the different cases compared to base case with air as gasifying medium.

Variable	**Case**		
	Base case, air as gasifying medium	**Same lambda, 21% O_2**	**Same lambda and total flow, 29.5% O_2**
Gasifying medium flow rate (kg/h)	1148	1651	1148
Temperature (°C)	878	781	859
Tar flow rate (kg/h)	8.43	9.84	8.70
LHV ex. tars (MJ/Nm^3)	6.63	6.83	8.08
LHV inc. tars (MJ/Nm^3)	6.83	7.10	8.34
CGE inc. tars (-)	0.77	0.72	0.74
Separation eff. (%)	99.4	99.6	99.6
Unreacted char (kg/h)	20.99	40.29	36.19
Dry syngas flow (Nm^3/h)	1585	1423	1247
vol.% H_2O (wb)	11.2	17.5	17.1

The last case presented is obtained by employing an optimization block in Aspen Plus®. The objective function set to be maximized is the CGE of the process. Only one constraint was defined, the temperature should not exceed 1000 °C. The manipulated variables allowed to be varied are mass flows of O_2 and CO_2. The result is a setup with an oxidant stream of pure O_2 at 226 kg/h resulting in a syngas with 12.8 vol.% water, 904 Nm^3/h in gas flow, LHV of 11.90 MJ/Nm^3 ex. tars, LHV of 12.19 MJ/Nm^3 inc. tars, 7.15 kg/h tars and 34.4 kg/h unreacted char. The calculated reactor temperature was 963 °C with a CGE of 0.78. The pressure drop calculated was 49 mbar with a particle separation efficiency of 99.7%.

Main components of syngas produced in this case are shown in Figure 5.17 as mol component per a unit of dry ash-free fuel ($mol/kg_{F,daf}$). The predicted gas composition on dry basis for this case is presented in Figure 5.18. It must be pointed out that this case was simulated for demonstration purpose to show the maximum CGE possible to achieve without taking cyclone separation in consideration. The cyclone separation will definitely be affected as the gas volumetric flow rate is much lower in this case compared to the other cases presented previously. Therefore, further investigation about particle separation should be done if lower CO_2 fractions are to be used.

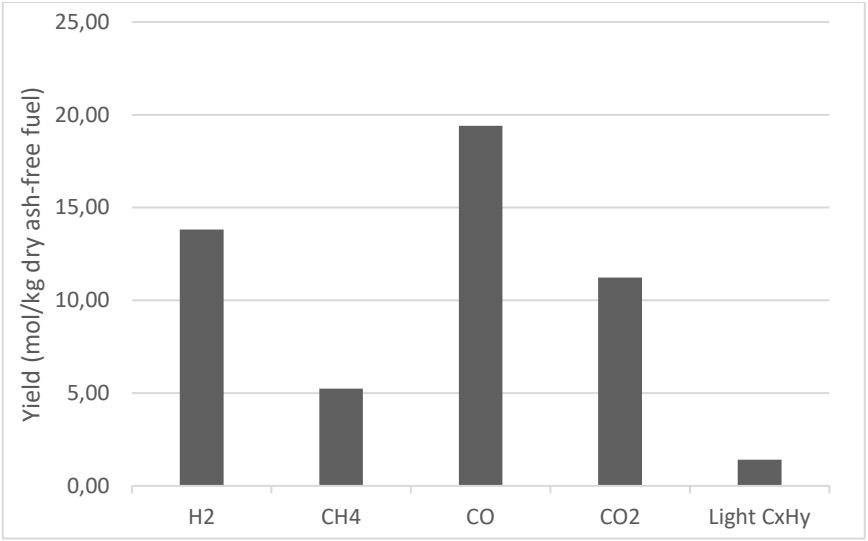

Figure 5.17. Predicted gas yields ($mol/kg_{F,daf}$) when 773 kg/h biomass was gasified with 226 kg/h gasifying medium consisting of pure O_2.

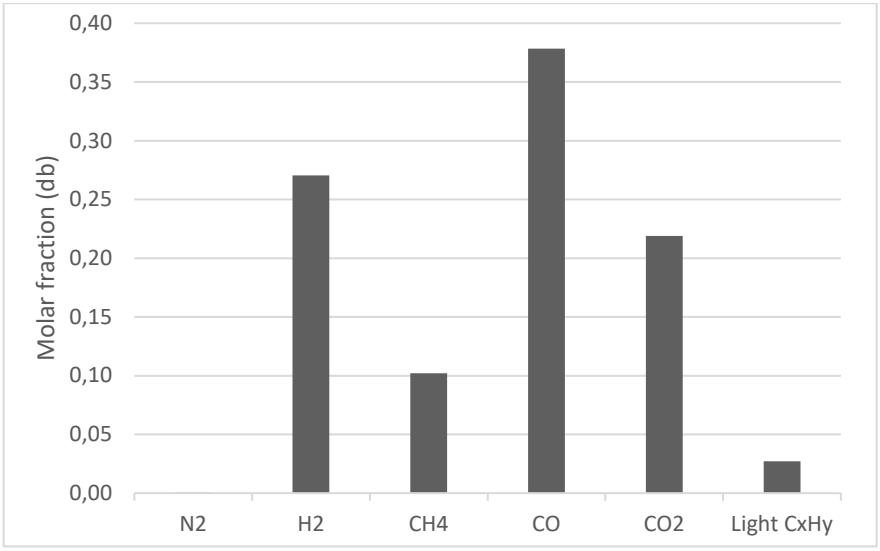

Figure 5.18. Predicted dry syngas molar composition when 773 kg/h biomass was gasified with 226 kg/h gasifying medium consisting of pure O_2.

Regarding the cases where N_2 is replaced with CO_2, a lower gasification temperature is observed compared to conventional air-blown gasification at the same lambda. There are two main explanations for this trend. Air has a lower specific heat capacity than the O_2/CO_2 mixture. For example. the mixture of 21 mol.% O2 and 79 mol.% CO2 at 900 °C has a specific heat capacity about 8% higher than corresponding value for air [31].

The other explanation is increased concentration of CO_2 will cause more carbon to react in the endothermic reaction 11 shown in Table 2.1. However, factorial experiments should be done to make conclusions about this effect, as the temperature variation due to change in specific heat capacity will affect the reaction rate also.

A low lambda value is desirable from an economical perspective of view as pure O_2 is expensive. The problem with keeping lambda value low is that the temperature drops a lot, therefore, it is important to keep the lambda value at around 0.3 depending on how much CO_2 is recirculated. A lower lambda value can be used if less CO_2 is recirculated as the temperature will increase. Unfortunately, enough particle separation in the cyclone cannot be guaranteed as the inlet velocity and physical properties of the gas mixture will change significantly. Another approach is considering preheating of recirculated CO_2 by utilizing waste heat, in this way less energy is consumed to heat CO_2 which will allow higher gasification temperature.

A lower tar mass flow is observed in cases with higher temperature. This is predicted by equations presented in Section 5.2, and as mentioned in Section 2.2, higher temperature allows more tars to crack. Regarding the LHV of product gas, a higher value is observed in second case due to lower CO_2 fraction.

6 Conclusions

As of today, most simulations in Aspen Plus® found in literature are based on equilibrium models. Common for most equilibrium models is the overestimation of char conversion and the neglect of tars and their reactions during gasification. However, some authors used kinetic expressions and correlations to develop more accurate models in Aspen Plus®. In this study, two different models have been developed, one model fully equilibrium-based, and another model based on equilibrium with kinetics and correlations found in literature.

Collection of relevant process flow diagrams, technical specifications of operating units and measurement data from the existing gasification plant have been done. Subsequent biological methanation of produced syngas has been studied to define requirements on the biomass gasification. A syngas free of N_2, low tar content and a temperature within 50–100 °C after the gas-cleaning system is required for the biological methanation. Furthermore, high content of H_2, CH_4 and CO is desired to reach higher syngas conversion and process efficiency.

Results from the equilibrium model showed almost no agreement with experimental data. The predicted temperature is much lower, large deviations are found in concentrations of main components, and tars were neglected. However, the sensitivity analysis showed the same trends as experimental data except for CO_2 and light non-aromatic hydrocarbons when mass flow of air was varied.

Results from the kinetic model showed much better agreement with experimental data, however, still some deviations are observed in the gas yields. Sensitivity analysis of this model showed better agreement when air mass flow rate was varied, but still some deviations were observed in yields of CH_4 and light non-aromatic hydrocarbons. When the moisture content of biomass was changed, the kinetic-based model could successfully predict similar trends in syngas composition as shown by experimental data for most components. Both models overestimated CGE of the process and underestimated tar content of produced syngas.

The gas-cleaning system was also modeled and simulated in a third model. Validation of this model showed some agreement with experimental data. However, big errors for some components such as indene and naphthalene were observed in the final gas composition. This model could be useful to study which operating units are most important as experimental data of the tar content between operating units are not available. However, this model would not be able to predict how the different operating units will behave when operating conditions are changed from the base case.

Finally, the kinetic-based model was then used to adapt gasification of biomass to the biological methanation. This was done by setting up some criteria such as replacement of N_2 in air with recirculated CO_2 obtaining similar temperature. No comprehensive optimization was carried out, but two initial setups were proposed. For all setups presented, a lower gasification temperature is predicted with a decrease in CGE but with higher LHV of produced syngas.

6.1 Future work

Several improvements could be made to the model developed in this study. The main improvement should be done in modeling of the heterogeneous reactions of char. A kinetic model should replace the equilibrium model with all reactions in the same block in Aspen Plus®. If no kinetic expression can be developed, then an alternative approach is to conduct experiments to set correct temperature restriction for the heterogeneous reactions. One more important improvement is the introduction of more tar components than benzene produced in the pyrolysis step. These improvements would result in a more accurate model causing less deviations from experimental data.

Modeling of interaction between tars and particles would improve the simulation of the gas-cleaning process. Furthermore, the implementation of a particle growth model would make the simulation of particle separation more accurate. Especially if a custom Aspen Plus® model is developed with reactions in a cyclone instead of a CSTR as size of particles decreases in the gasifier.

If biomass with higher nitrogen and/or sulfur content is used, then modeling of the components of these elements should be done. These elements can form toxic contaminants to the microorganisms used in biological methanation of syngas. This improvement to the model would allow the investigation of different biomasses with analysis of their suitability to the biological methanation.

Finally, a comprehensive optimization of the gasifier must be done when adapting it to biological methanation of syngas. A techno-economic analysis of this adaptation should also be performed, considering the increased operating costs due to utilization of pure O_2 instead of air. Moreover, the effect of lower gasifying medium flow rate on cyclone particle separation efficiency should also be considered.

7 References

[1] "About us - Meva Energy Home Page." https://mevaenergy.com/about-us/ (accessed Nov 26, 2021).

[2] A. Wingren, "Personal communication," A. Almashharawi, Ed., ed. Lund, Sweden: RISE AB, 2021.

[3] M. A. Chishty, K. Umeki, M. Risberg, A. Wingren, and R. Gebart, "Numerical simulation of a biomass cyclone gasifier: Effects of operating conditions on gasifier performance," *Fuel Process. Technol.,* vol. 218, p. 106861, 2021, doi: https://doi.org/10.1016/j.fuproc.2021.106861.

[4] D. Neves, H. Thunman, A. Matos, L. Tarelho, and A. Gómez-Barea, "Characterization and prediction of biomass pyrolysis products," *Prog. Energy Combust. Sci.,* vol. 37, no. 5, pp. 611-630, 2011, doi: https://doi.org/10.1016/j.pecs.2011.01.001.

[5] M. Risberg, "Entrained flow gasification of biomass : On atomisation, transport processes and gasification reactions," Doctoral thesis, comprehensive summary, Doctoral thesis / Luleå University of Technology 1 jan 1997 → …, Luleå tekniska universitet, Luleå, 2013. [Online]. Available: http://urn.kb.se/resolve?urn=urn:nbn:se:ltu:diva-18740

[6] "Biogas - Clarke Energy Home Page." https://www.clarke-energy.com/applications/biogas/ (accessed Dec 01, 2021).

[7] "Biologisk metanisering av syngas från förgasning av lignocellulosa - RISE Home Page." https://www.ri.se/sv/vad-vi-gor/projekt/biologisk-metanisering-av-syngas-fran-forgasning-av-lignocellulosa (accessed Dec 01, 2021).

[8] J. Andersson, "Personal communication," A. Almashharawi, Ed., ed. Uppsala, Sweden: RISE AB, 2021.

[9] S. Youngsukkasem, K. Chandolias, and M. J. Taherzadeh, "Rapid bio-methanation of syngas in a reverse membrane bioreactor: Membrane encased microorganisms," *Bioresour. Technol.,* vol. 178, pp. 334-340, 2015, doi: https://doi.org/10.1016/j.biortech.2014.07.071.

[10] H. Olsson, "Personal communication," A. Almashharawi, Ed., ed. Uppsala, Sweden: RISE AB, 2021.

[11] R. Timsina, R. Thapa, and M. Eikeland, "Aspen Plus simulation of biomass gasification for different types of biomass," in *Proceedings of The 60th SIMS Conference on Simulation and Modelling (SIMS 60)*, Västerås, Sweden, 2019, doi: https://doi.org/10.3384/ecp20170151.

[12] M. Eikeland, R. Thapa, and B. Halvorsen, "Aspen Plus Simulation of Biomass Gasification with Known Reaction Kinetic," in *Proceedings of The 56th SIMS Conference on Simulation and Modelling (SIMS 56)*, Linköping, Sweden, 2015, doi: http://dx.doi.org/10.3384/ecp15119149.

[13] I. Adeyemi and I. Janajreh, "Modeling of the entrained flow gasification: Kinetics-based ASPEN Plus model," *Renewable Energy,* vol. 82, pp. 77-84, 2015, doi: https://doi.org/10.1016/j.renene.2014.10.073.

[14] M. Puig-Gamero, J. Argudo-Santamaria, J. L. Valverde, P. Sánchez, and L. Sanchez-Silva, "Three integrated process simulation using aspen plus®: Pine gasification, syngas cleaning and methanol synthesis," *Energy Convers. Manage.,* vol. 177, pp. 416-427, 2018, doi: https://doi.org/10.1016/j.enconman.2018.09.088.

[15] M. B. Nikoo and N. Mahinpey, "Simulation of biomass gasification in fluidized bed reactor using ASPEN PLUS," *Biomass Bioenergy,* vol. 32, no. 12, pp. 1245-1254, 2008, doi: https://doi.org/10.1016/j.biombioe.2008.02.020.

[16] N. Ramzan, A. Ashraf, S. Naveed, and A. Malik, "Simulation of hybrid biomass gasification using Aspen plus: A comparative performance analysis for food, municipal solid and poultry waste," *Biomass Bioenergy,* vol. 35, no. 9, pp. 3962-3969, 2011, doi: https://doi.org/10.1016/j.biombioe.2011.06.005.

[17] M. Niu, Y. Huang, B. Jin, and X. Wang, "Simulation of Syngas Production from Municipal Solid Waste Gasification in a Bubbling Fluidized Bed Using Aspen Plus," *Industrial & Engineering Chemistry Research,* vol. 52, no. 42, pp. 14768-14775, 2013, doi: https://doi.org/10.1021/ie400026b.

[18] S. Begum, M. G. Rasul, and D. Akbar, "A Numerical Investigation of Municipal Solid Waste Gasification Using Aspen Plus," *Procedia Engineering,* vol. 90, pp. 710-717, 2014, doi: https://doi.org/10.1016/j.proeng.2014.11.800.

[19] J. Han *et al.*, "Modeling downdraft biomass gasification process by restricting chemical reaction equilibrium with Aspen Plus," *Energy Convers. Manage.,* vol. 153, pp. 641-648, 2017, doi: https://doi.org/10.1016/j.enconman.2017.10.030.

[20] P. Kaushal and R. Tyagi, "Advanced simulation of biomass gasification in a fluidized bed reactor using ASPEN PLUS," *Renewable Energy,* vol. 101, pp. 629-636, 2017, doi: https://doi.org/10.1016/j.renene.2016.09.011.

[21] A. Gagliano, F. Nocera, M. Bruno, and G. Cardillo, "Development of an Equilibrium-based Model of Gasification of Biomass by Aspen Plus," *Energy Procedia,* vol. 111, pp. 1010-1019, 2017, doi: https://doi.org/10.1016/j.egypro.2017.03.264.

[22] Y. Cao, Q. Wang, J. Du, and J. Chen, "Oxygen-enriched air gasification of biomass materials for high-quality syngas production," *Energy Convers. Manage.,* vol. 199, p. 111628, 2019, doi: https://doi.org/10.1016/j.enconman.2019.05.054.

[23] Ö. Ç. Mutlu and T. Zeng, "Challenges and Opportunities of Modeling Biomass Gasification in Aspen Plus: A Review," *Chemical Engineering & Technology,* vol. 43, no. 9, pp. 1674-1689, 2020, doi: https://doi.org/10.1002/ceat.202000068.

[24] M. Risberg, P. Carlsson, and R. Gebart, "Numerical modeling of a 500 kW air-blown cyclone gasifier," *Appl. Therm. Eng.,* vol. 90, pp. 694-702, 2015, doi: https://doi.org/10.1016/j.applthermaleng.2015.06.056.

[25] S. S. Hla, D. G. Roberts, and D. J. Harris, "A numerical model for understanding the behaviour of coals in an entrained-flow gasifier," *Fuel Process. Technol.,* vol. 134, pp. 424-440, 2015, doi: https://doi.org/10.1016/j.fuproc.2014.12.053.

[26] I. Adeyemi, I. Janajreh, T. Arink, and C. Ghenai, "Gasification behavior of coal and woody biomass: Validation and parametrical study," *Applied Energy,* vol. 185, pp. 1007-1018, 2017, doi: https://doi.org/10.1016/j.apenergy.2016.05.119.

[27] E. Karampinis, N. Nikolopoulos, A. Nikolopoulos, P. Grammelis, and E. Kakaras, "Numerical investigation Greek lignite/cardoon co-firing in a tangentially fired furnace," *Applied Energy,* vol. 97, pp. 514-524, 2012, doi: https://doi.org/10.1016/j.apenergy.2011.12.032.

[28] "Computer Models Reduce the Need for Real-World Testing in Chemical Process Engineering - CHEManager Home Page." https://www.chemanager-online.com/en/news/modelling-and-simulation (accessed Nov 30, 2021).

[29] L. Vaquerizo and M. J. Cocero, "CFD–Aspen Plus interconnection method. Improving thermodynamic modeling in computational fluid dynamic simulations," *Computers & Chemical Engineering,* vol. 113, pp. 152-161, 2018, doi: https://doi.org/10.1016/j.compchemeng.2018.03.019.

[30] S. E. Zitney and M. Syamlal, "Integrated Process Simulation and CFD for Improved Process Engineering," in *Computer Aided Chemical Engineering*, vol. 10, J. Grievink and J. van Schijndel Eds.: Elsevier, 2002, pp. 397-402.
[31] M. Alveteg, Ed. *Handbook: Physical Properties, Correlations and Equations in Chemical Engineering*. Department of Chemical Engineering, Faculty of Engineering, 2021.
[32] *Aspen Plus - Getting Started Modeling Processes with Solids*. (2013).
[33] J. Ritvanen, K. Myöhänen, A. Pitkäoja, and T. Hyppänen, "Modeling of industrial-scale sorption enhanced gasification process: One-dimensional simulations for the operation of coupled reactor system," *Energy,* vol. 226, p. 120387, 2021, doi: https://doi.org/10.1016/j.energy.2021.120387.
[34] A. Almoslh, F. Alobaid, C. Heinze, and B. Epple, "Comparison of Equilibrium-Stage and Rate-Based Models of a Packed Column for Tar Absorption Using Vegetable Oil," *Applied Sciences,* vol. 10, no. 7, 2020, doi: https://doi.org/10.3390/app10072362.
[35] H. Gai, L. Qiao, C. Zhong, X. Zhang, M. Xiao, and H. Song, "A solvent based separation method for phenolic compounds from low-temperature coal tar," *Journal of Cleaner Production,* vol. 223, pp. 1-11, 2019, doi: https://doi.org/10.1016/j.jclepro.2019.03.102.
[36] T. Jiao, C. Li, X. Zhuang, S. Cao, H. Chen, and S. Zhang, "The new liquid–liquid extraction method for separation of phenolic compounds from coal tar," *Chem. Eng. J.,* vol. 266, pp. 148-155, 2015, doi: https://doi.org/10.1016/j.cej.2014.12.071.
[37] T. Jiao, X. Qin, H. Zhang, W. Zhang, Y. Zhang, and P. Liang, "Separation of phenol and pyridine from coal tar via liquid–liquid extraction using deep eutectic solvents," *Chem. Eng. Res. Des.,* vol. 145, pp. 112-121, 2019, doi: https://doi.org/10.1016/j.cherd.2019.03.006.
[38] T. Jiao *et al.*, "An ionic liquid extraction process for the separation of indole from wash oil," *Green Chemistry,* 10.1039/C5GC00081E vol. 17, no. 7, pp. 3783-3790, 2015, doi: http://dx.doi.org/10.1039/C5GC00081E.
[39] X. Zhang *et al.*, "COSMO-based solvent selection and Aspen Plus process simulation for tar absorptive removal," *Applied Energy,* vol. 251, p. 113314, 2019, doi: https://doi.org/10.1016/j.apenergy.2019.113314.

8 List of abbreviations

ΔH_{vap}	Enthalpy of vaporization (MJ/kg)
C	Elemental Carbon
C_2H_2	Ethyne
C_2H_4	Ethylene
C_2H_6	Ethane
C6H6	Benzene
CFD	Computational Fluid Dynamic
CGE	Cold gas efficiency
CH_4	Methane
Cl	Elemental Chlorine
Cl_2	Chlorine gas
CO	Carbon monoxide
CO_2	Carbon dioxide
CSTR	Continuous stirred-tank reactor
daf	dry ash-free basis
db	dry basis
F	Fuel
FC	Fixed carbon
H	Elemental hydrogen
H_2	Hydrogen gas
H_2O	Water
HHV	Higher heating value (MJ/kg)
LHV	Lower heating value (MJ/Nm^3)
m_i	Mass flow rate of component (kg i/h)
N	Elemental nitrogen

N_2	Nitrogen gas
NRTL	Non-random two-liquid
O	Elemental oxygen
O_2	Oxygen gas
PAHs	Polycyclic aromatic hydrocarbons
PR	Peng Robinson cubic equation of state
PR-BM	Peng Robinson cubic equation of state with the Boston-Mathias alpha function
PSD	Particle size distribution
Q_{RSTOIC}	Heat produced by combustion reactions (MJ)
RK-SOAVE	Soave-Redlich-Kwong equation of state
S	Elemental sulfur
T	Temperature (°C)
V_i	Volumetric flow rate of component i (m^3 i/h)
VM	Volatile matter
wb	Wet basis
WESP	Wet electrostatic precipitator
wt.%	weight percentage
$y_{i,F}$	Yield of component i (kg i/kg dry ash-free fuel)
$y_{i,j}$	Mass fraction of element i in component j (kg i/kg j)s